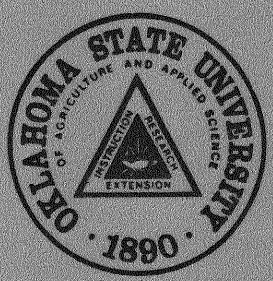

SCHOOL OF CIVIL ENGINEERING OKLAHOMA STATE UNIVERSITY

FINAL REPORT

FATIGUE DAMAGE TO STEEL BRIDGE DIAPHRAGMS

By
Farrel J. Zwerneman
Adam B. West
Kee Seong Lim

Report No. FHWA/OK 89(10)
December, 1989

TECHNICAL REPORT STANDARD TITLE PAGE

1. REPORT NO.	2. GOVERNMENT ACCESSION NO.	3. RECIPIENT'S CATALOG NO.
FHWA/OK 89(10)		

4. TITLE AND SUBTITLE

FATIGUE DAMAGE TO STEEL BRIDGE DIAPHRAGMS

5. REPORT DATE
December, 1989

6. PERFORMING ORGANIZATION CODE

7. AUTHOR(S)
Farrel J. Zwerneman
Adam B. West
Kee Seong Lim

8. PERFORMING ORGANIZATION REPORT
89-10

10. WORK UNIT NO.

9. PERFORMING ORGANIZATION AND ADDRESS
School of Civil Engineering
Oklahoma State University
Stillwater, OK 74078-0327

11. CONTRACT OR GRANT NO.
2156

13. TYPE OF REPORT AND PERIOD COVERED
Final Report: 4/1/87-12/31/89

12. SPONSORING AGENCY NAME AND ADDRESS
Oklahoma Department of Transportation
Research and Development Division
200 NE 21st Street
Oklahoma City, OK 73105

14. SPONSORING AGENCY CODE
Item 2156

15. SUPPLEMENTARY NOTES
Conducted in cooperation with U.S. Department of Transportation, Federal Highway Administration

16. ABSTRACT

The cause of diaphragm cracking on an interstate highway bridge was investigated. The investigation consisted of load-testing the bridge, performing a computer-aided analysis of the bridge superstructure and specific components, measuring the chemical and physical properties of the diaphragm steel, and performing fatigue tests on simulated diaphragms.

It was determined that the high degree of restraint at the diaphragm-to-girder connection causes individual diaphragms at each transverse location to act as continuous members reaching from one side of the bridge to the other. Differential deflections of longitudinal members induce moments in the diaphragms, resulting in tensile stresses along the bottom of the diaphragms. These tensile stresses are amplified by the presence of a bottom-flange cope at the diaphragm-to-girder connections. High tensile stresses lead to initiation of fatigue cracks in diaphragms at copes.

A number of repair techniques were tested. These include attaching an auxiliary flange, smoothing out the cope, reducing restraint in the connection by removing bolts from the connection, and replacing coped diaphragms with uncoped diaphragms. The technique of removing bolts from the connection is recommended for implementation since it is by far the simplest to perform and is effective in extending fatigue life.

17. KEY WORDS	18. DISTRIBUTION STATEMENT
Fatigue, Bridge Diaphragms, Flange Copes	No Restrictions

19. SECURITY CLASSIF. (OF THIS REPORT)	20. SECURITY CLASSIF. (OF THIS PAGE)	21. NO. OF PAGES	22. PRICE
None	None	68	

FATIGUE DAMAGE TO STEEL BRIDGE DIAPHRAGMS

State Study No. 2156

Final Report

By

Farrel J. Zwerneman
Adam B. West
and
Kee Seong Lim

Prepared as part of an investigation
conducted by the
School of Civil Engineering
Oklahoma State University
in cooperation with the
Research and Development Division
Oklahoma Department of Transportation
State of Oklahoma
and the Federal Highway Administration
December, 1989

The contents of this report reflect the views of the author who is responsible for the facts and the accuracy of the data presented herein. The contents do not necessarily reflect the official views of the Oklahoma Department of Transportation or the Federal Highway Administration. This report does not constitute a standard, specification, or regulation. While equipment and contractor names are used in this report, it is not intended as an endorsement of any machine, contractor, or product.

EXECUTIVE SUMMARY

The cause of diaphragm cracking on an interstate highway bridge was investigated. The investigation consisted of load-testing the bridge, performing a computer-aided analysis of the bridge superstructure and specific components, measuring the chemical and physical properties of the diaphragm steel, and performing fatigue tests on simulated diaphragms.

It was determined that the high degree of restraint at the diaphragm-to-girder connection causes individual diaphragms at each transverse location to act as continuous members reaching from one side of the bridge to the other. Differential deflections of longitudinal members induce moments in the diaphragms, resulting in tensile stresses along the bottom of the diaphragms. These tensile stresses are amplified by the presence of a bottom-flange cope at the diaphragm-to-girder connections. High tensile stresses lead to initiation of fatigue cracks in diaphragms at copes.

A number of repair techniques were tested. These include attaching an auxiliary flange, smoothing out the cope, reducing restraint in the connection by removing bolts from the connection, and replacing coped diaphragms with uncoped diaphragms. The technique of removing bolts from the connection is recommended for implementation since it is by far the simplest to perform and is effective in extending fatigue life.

ACKNOWLEDGMENTS

The investigation reported here was conducted as a project of Engineering Research at Oklahoma State University in the School of Civil Engineering under sponsorship of the Oklahoma Department of Transportation. The authors wish to thank all who contributed to the success of this investigation, especially the Oklahoma Department of Transportation personnel who assisted in the field work.

TABLE OF CONTENTS

LIST OF TABLES

LIST OF FIGURES

Figure | Page

CHAPTER 1

INTRODUCTION

1.1 Problem Statement

This research was conducted to identify the cause of diaphragm cracking in a steel girder highway bridge. The bridge, located on I-40 near Weatherford, Oklahoma, is shown in Figure 1. The bridge is about 20 years old and 60 of the 184 diaphragms in both the east and westbound spans are cracked, 5 of which have experienced a total section loss. A picture showing the position of several diaphragms on the bridge is presented in Figure 2, and two examples of fatigue damage are shown in Figure 3. In all but one case, cracks initiate at the lower flange and propagate up through the member. The one case where cracks were found in the upper cope is also the one case where cracks were found in diaphragms above pier caps. Locations of cracked diaphragms are indicated in Figure 4.

Damage to diaphragms does not pose an immediate threat to the integrity of the bridge; however, loss of the diaphragms will result in loss of support for the concrete deck and possibly accelerate normal deterioration of the deck. In addition, the American Association of State Highway and Transportation Officials (AASHTO), Standard Specifications for Highway Bridges [1], requires the presence of diaphragms at intervals not to exceed 25 ft.

Oklahoma Department of Transportation (ODOT) inspectors have noted similar problems at less advanced stages of cracking on other bridges. To reduce maintenance costs and to remain in compliance with specifications, the cause of the diaphragm cracking must be determined and an economically viable method of repair must be developed.

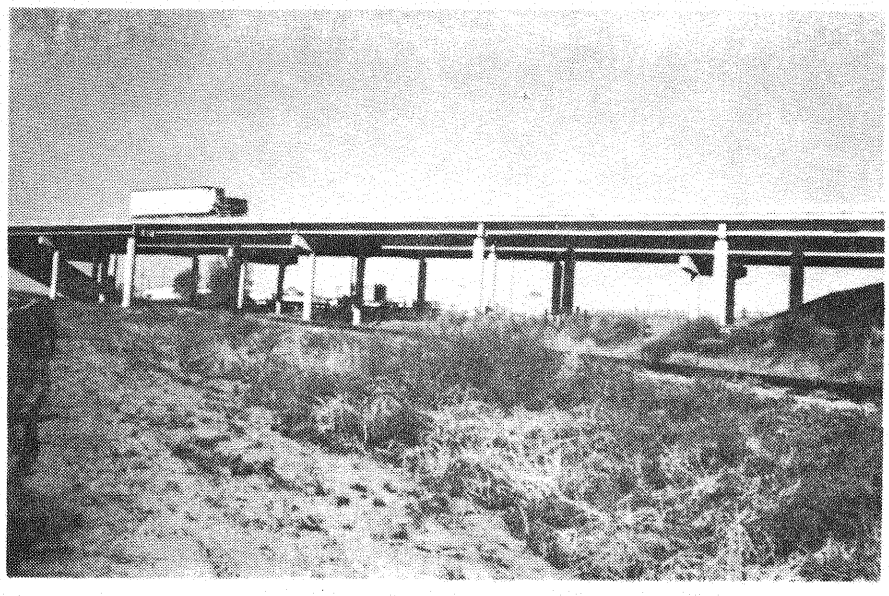

Figure 1. Bridge With Damaged Diaphragms, Structure No. 2004-1302SX

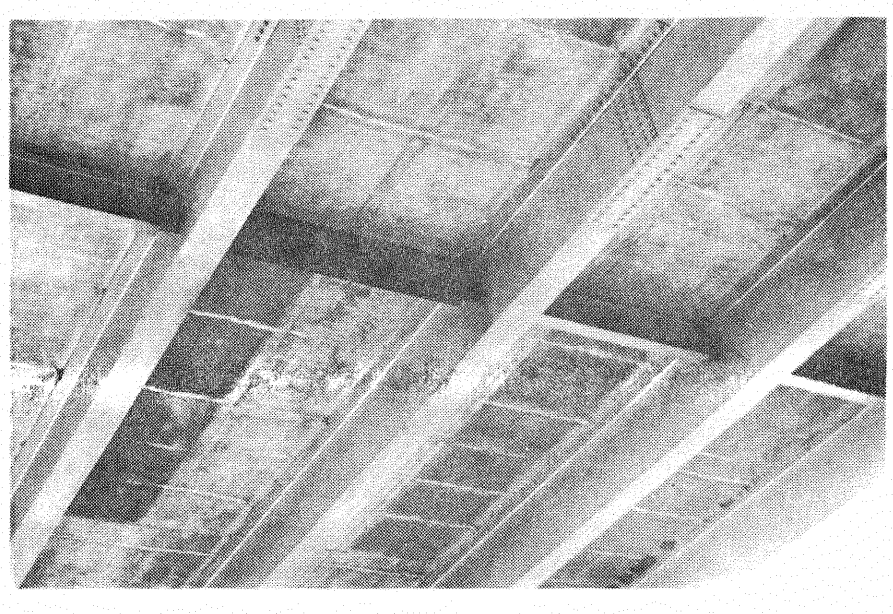

Figure 2. Position of Diaphragms

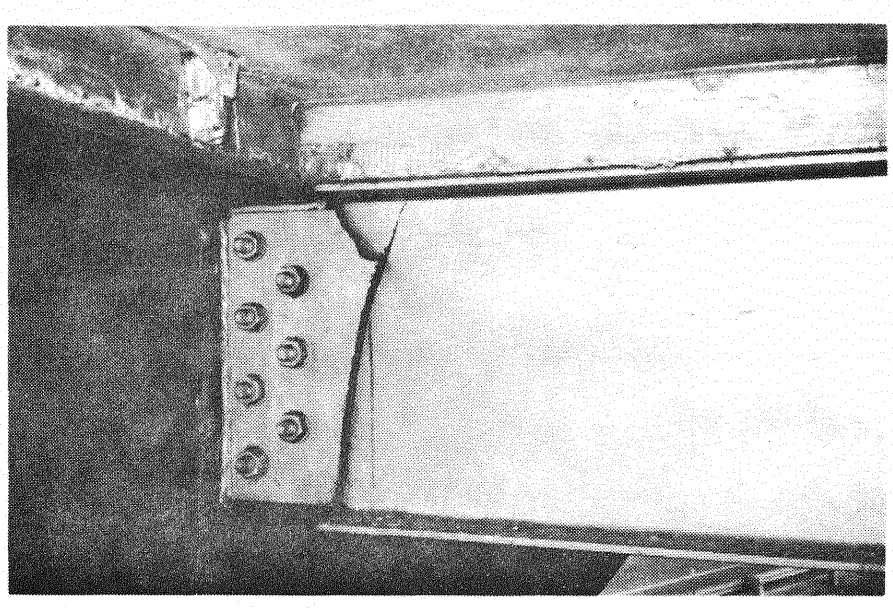

(a)

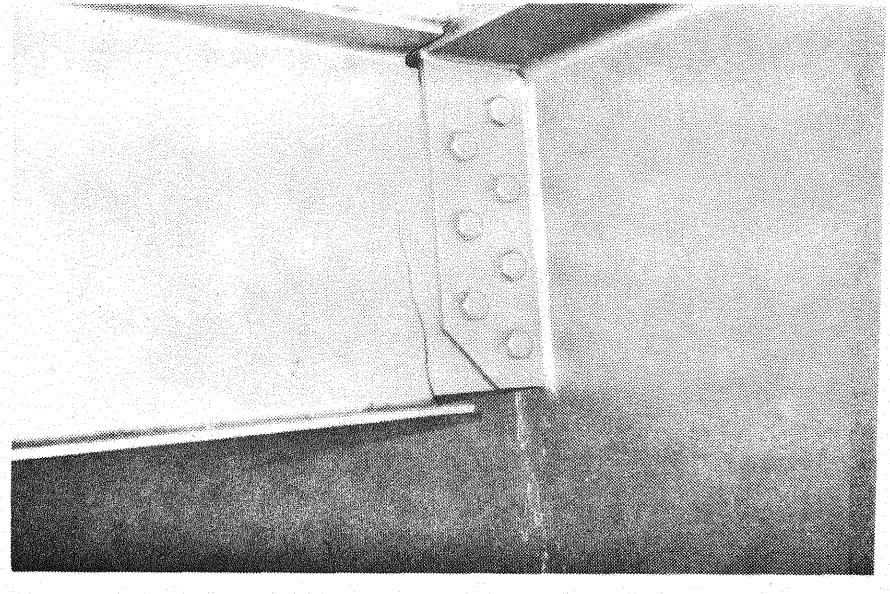

(b)

Figure 3. Examples of Cracked Diaphragms

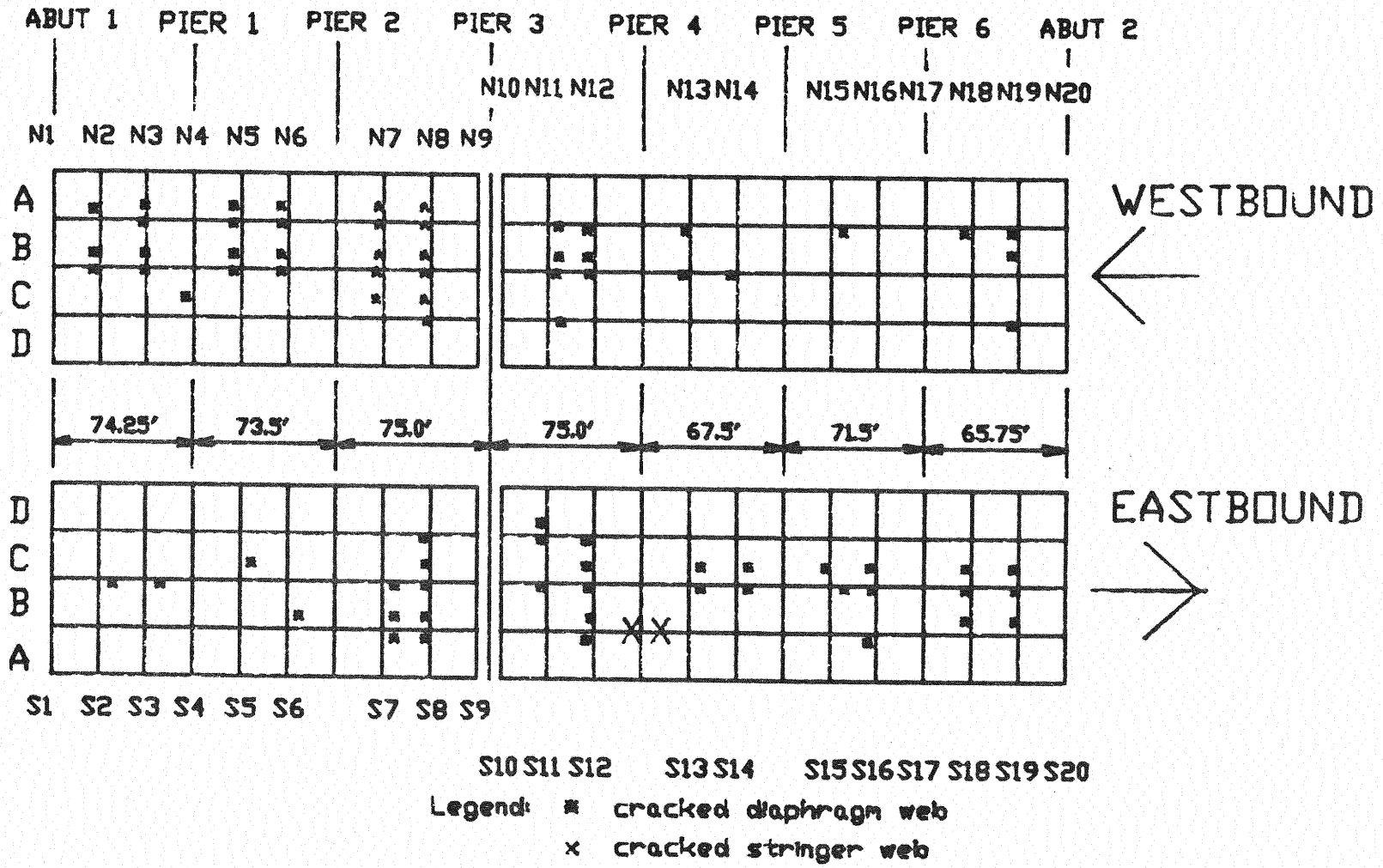

Figure 4. Plan View of Diaphragms and Stringers

1.2 Objectives

The objective of this research is to determine the cause of diaphragm cracking in the subject bridge and to propose an inexpensive method of repair. Once the cause of cracking in the subject bridge has been identified, the likelihood of the same problem occurring in other bridges and the suitability of the repair technique for these bridges can be assessed. A better understanding of the cause of diaphragm cracking in the subject bridge will also reduce the possibility of the same problem occurring in future construction.

1.3 Scope of Research

This research program involves instrumenting and testing the bridge under load, analyzing the entire bridge and isolated components of the bridge, developing methods for repairing damaged members, and testing these repair methods in the laboratory. To accomplish these tasks, three diaphragms were instrumented with strain gages and strains were recorded under a known truck weight. Analytical models of the bridge and diaphragm were developed to match measured strain distributions. Modifications which could be applied to actual diaphragms to improve their fatigue life were first applied to the analytical models to assess the impact of these modifications on the stress distribution in the diaphragm. Four different modifications were selected for testing under cyclic loads in the laboratory. To assess the effectiveness of the modifications, fatigue performance of modified diaphragms is directly compared to performance of unmodified diaphragms.

CHAPTER 2

FIELD TESTING

2.1 Instrumentation

This portion of the research involves the measurement of strains in diaphragms while the bridge is supporting a known load. A diaphragm fabricated to match the existing diaphragms was instrumented with strain gages at the Oklahoma State University Structural Laboratory. The instrumented diaphragm from the laboratory was used to replace the cracked diaphragm D2 shown in Figure 5. Details of the laboratory instrumented diaphragm are shown in Figure 6. Two other diaphragms, both without cracks, were instrumented in the field. These diaphragms are labeled D1 and D3 in Figure 5. The details of these diaphragms are shown in Figures 7 and 8. Measurement of differential displacements of longitudinal members in vertical and horizontal directions was also attempted during the field investigations but was not successful.

The majority of the data were taken with the bridge under static load. Data from diaphragm D2 were recorded using a 40-channel Vishay System 4000 under the control of an HP 9825 microcomputer. Data from diaphragms D1 and D3 were manually recorded using Measurements Group model SB-10 switch and balance units and model P-3500 portable strain indicators. The one set of data taken under dynamic load was recorded with the strain indicator connected to the y-axis of an x-y recorder and the x-axis set on a time scale. All strain gages had a resistance of 350 ohms and a length of 0.125 in.; rosette gages were Micro-Measurements model CEA-06-125UR-350 and single element gages were model CEA-06-125UW-350. Gages were connected to recording

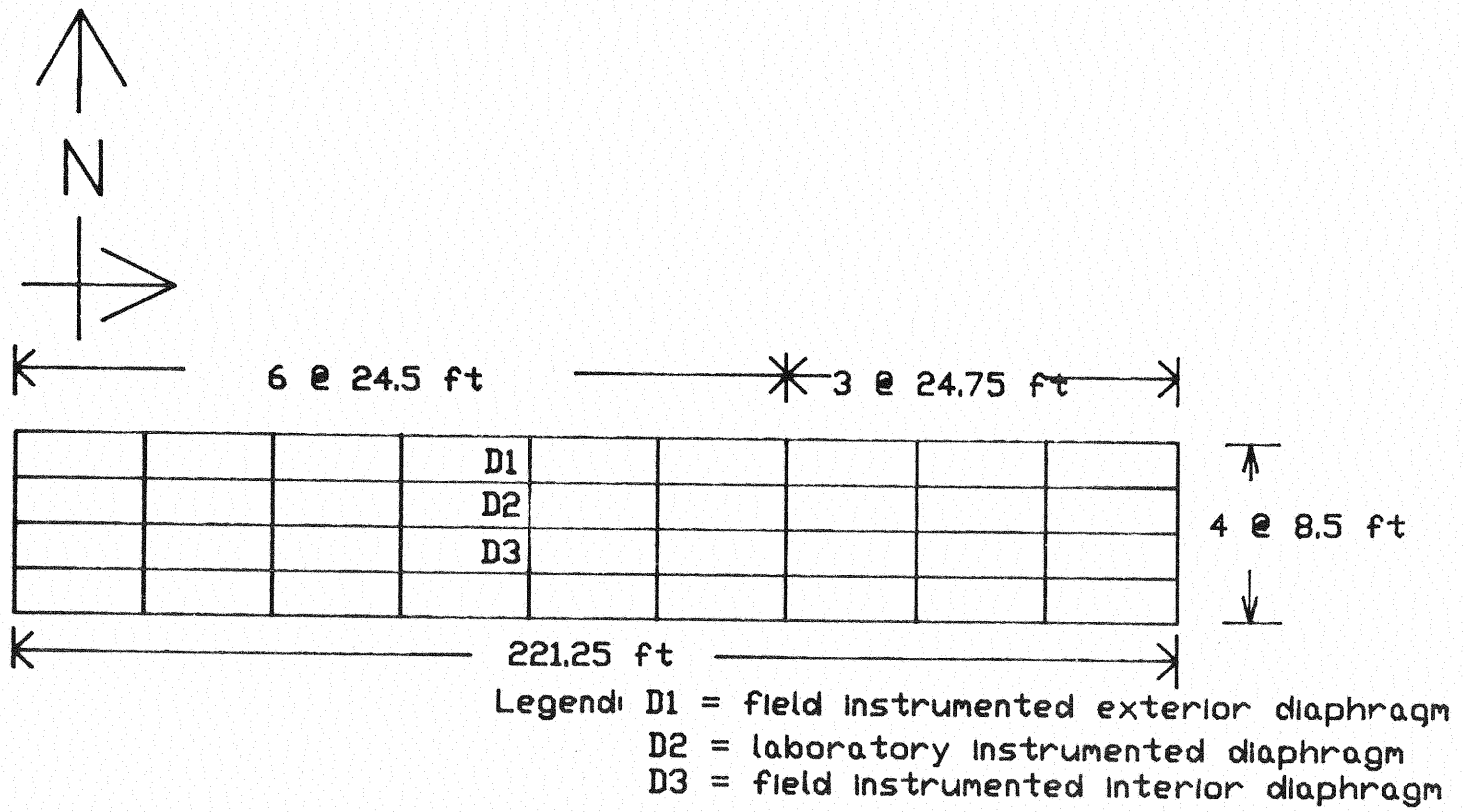

Figure 5. Location of Laboratory and Field Instrumented Diaphragms

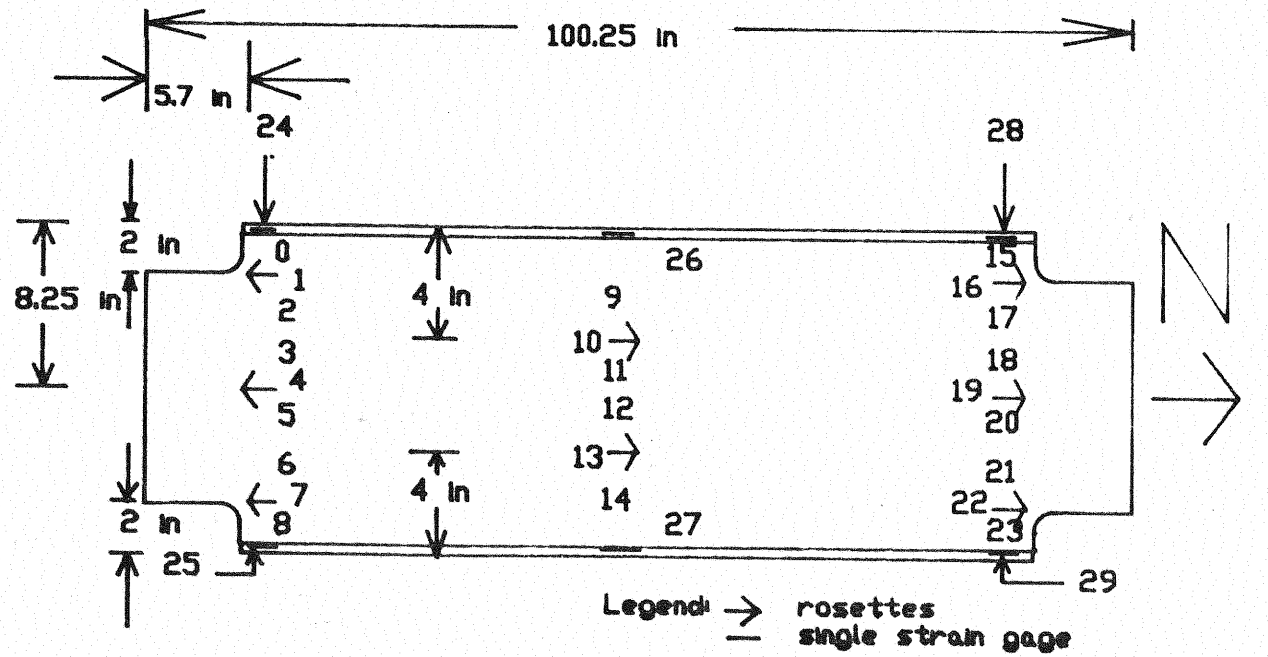

Figure 6. Location of Strain Gages on Laboratory Instrumented Diaphragm

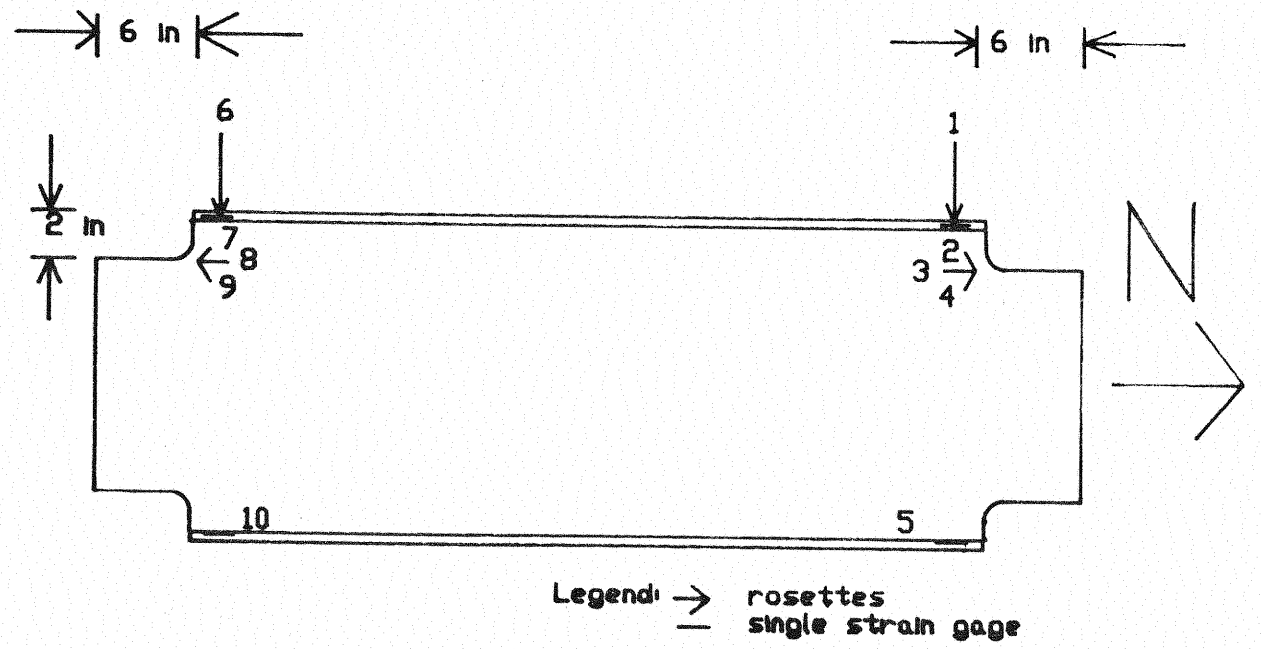

Figure 7. Location of Strain Gages on Field Instrumented Interior Diaphragm

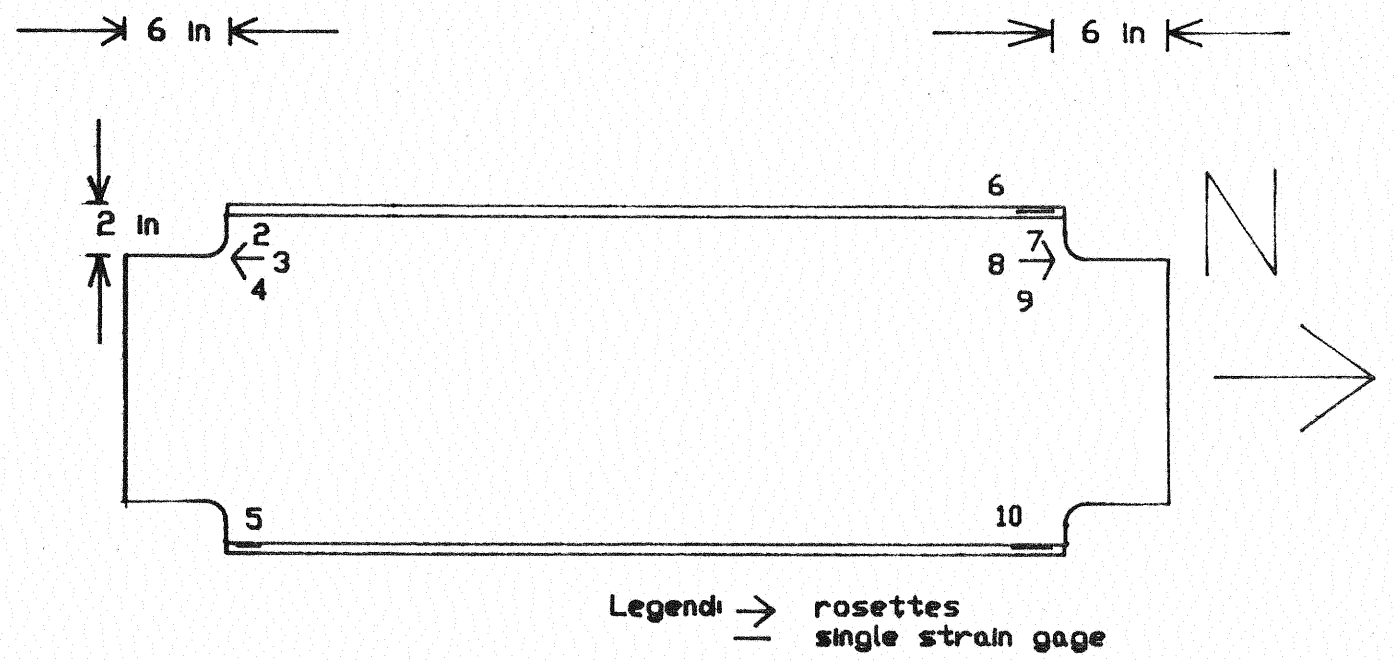

Figure 8. Location of Strain Gages on Field Instrumented Exterior Diaphragm

instruments using a three-conductor twisted cable with vinyl insulation, braided shield, and vinyl jacket.

2.2 Loading

The bridge was loaded with a tank truck supplied by ODOT. The truck is shown schematically in Figure 9. Strain measurements were taken for both lane and shoulder loading conditions. The location of the truck for the lane loading condition is shown in Figure 10 and for the shoulder loading condition in Figure 11. Only positions between abutment 1 and pier 3 (Figure 4) are shown in Figures 10 and 11. Strain measurements were taken for additional truck positions between pier 3 and abutment 2, but the truck had no effect on the instrumented diaphragm after it crossed pier 3, probably because longitudinal girders were not continuous across pier 3. To obtain static measurements, the truck was stopped at each numbered position and strains were recorded when the bridge was clear of all other traffic. Dynamic strain measurements were taken as the truck moved across the bridge at 20, 30, and 35 mph in the inside traffic lane.

2.3 Results

Plots of strain versus position of truck were prepared for each of the 50 strain gages installed on the three diaphragms for all lane and shoulder loading positions. Representative plots are shown in Figures 12 and 13. Figure 12 shows the values obtained at gage 22 for diaphragm D2 when the vehicle is located at various positions on the shoulder of the roadway. Figure 13 is a plot for gage 8 on diaphragm D1 for lane loading conditions.

As can be seen in Figures 12 and 13, strains produced by the truck are insignificant when the truck is on the spans preceding and following the span containing the instrumented diaphragms, even though longitudinal gir-

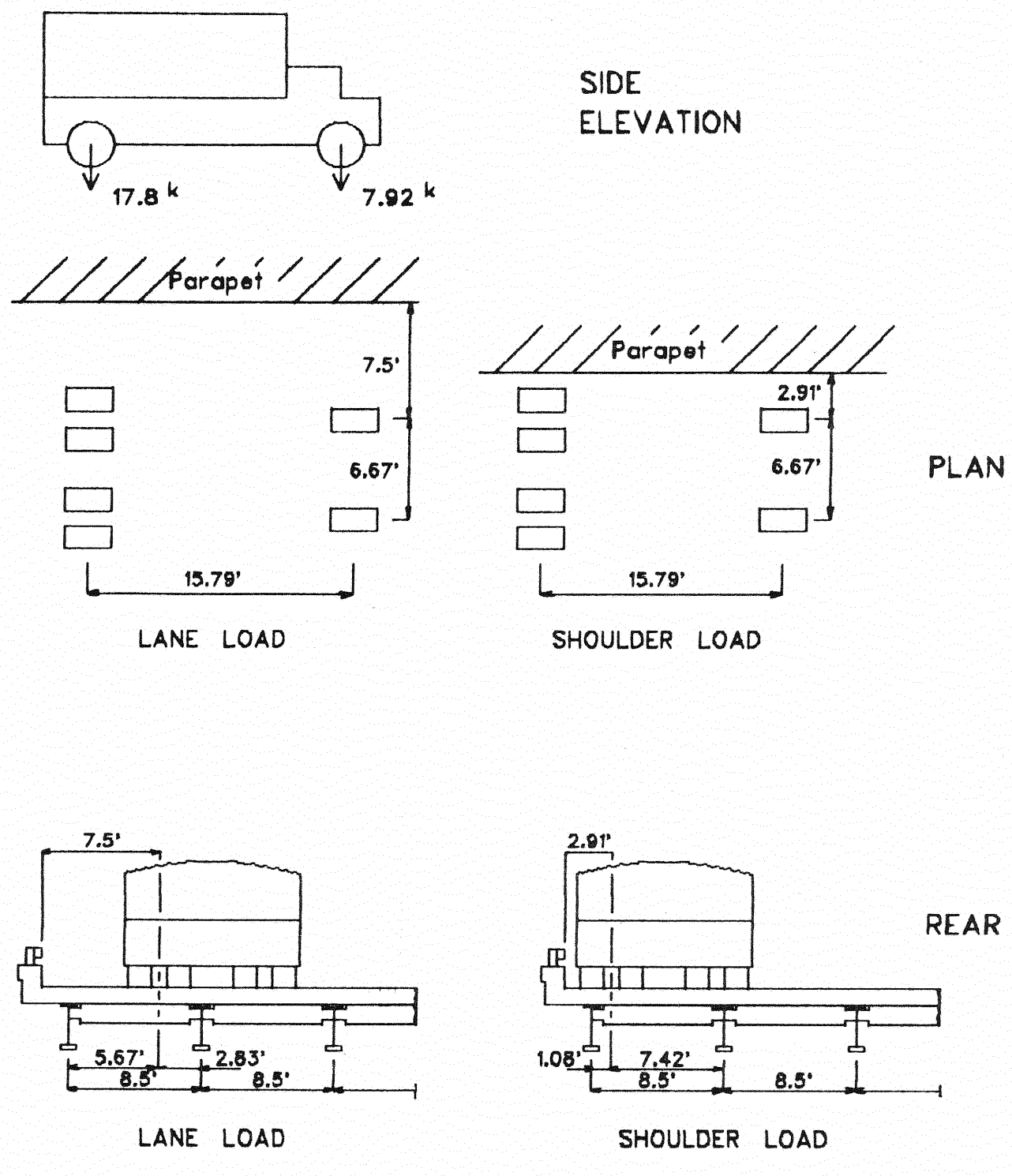

Figure 9. Tank Truck Used for Loading Bridge

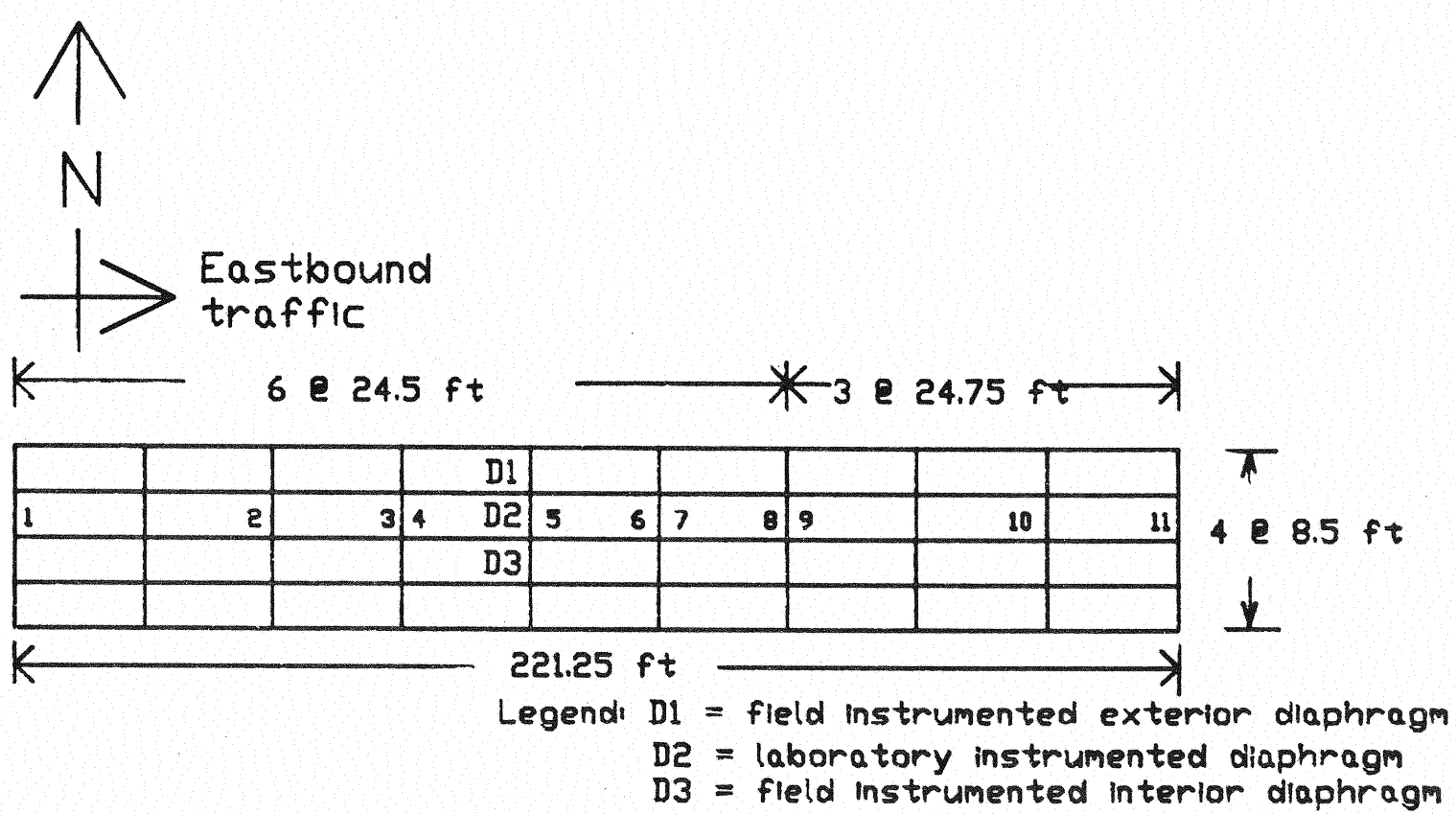

Figure 10. Lane Loadings at Various Positions Along First Three Spans of Bridge

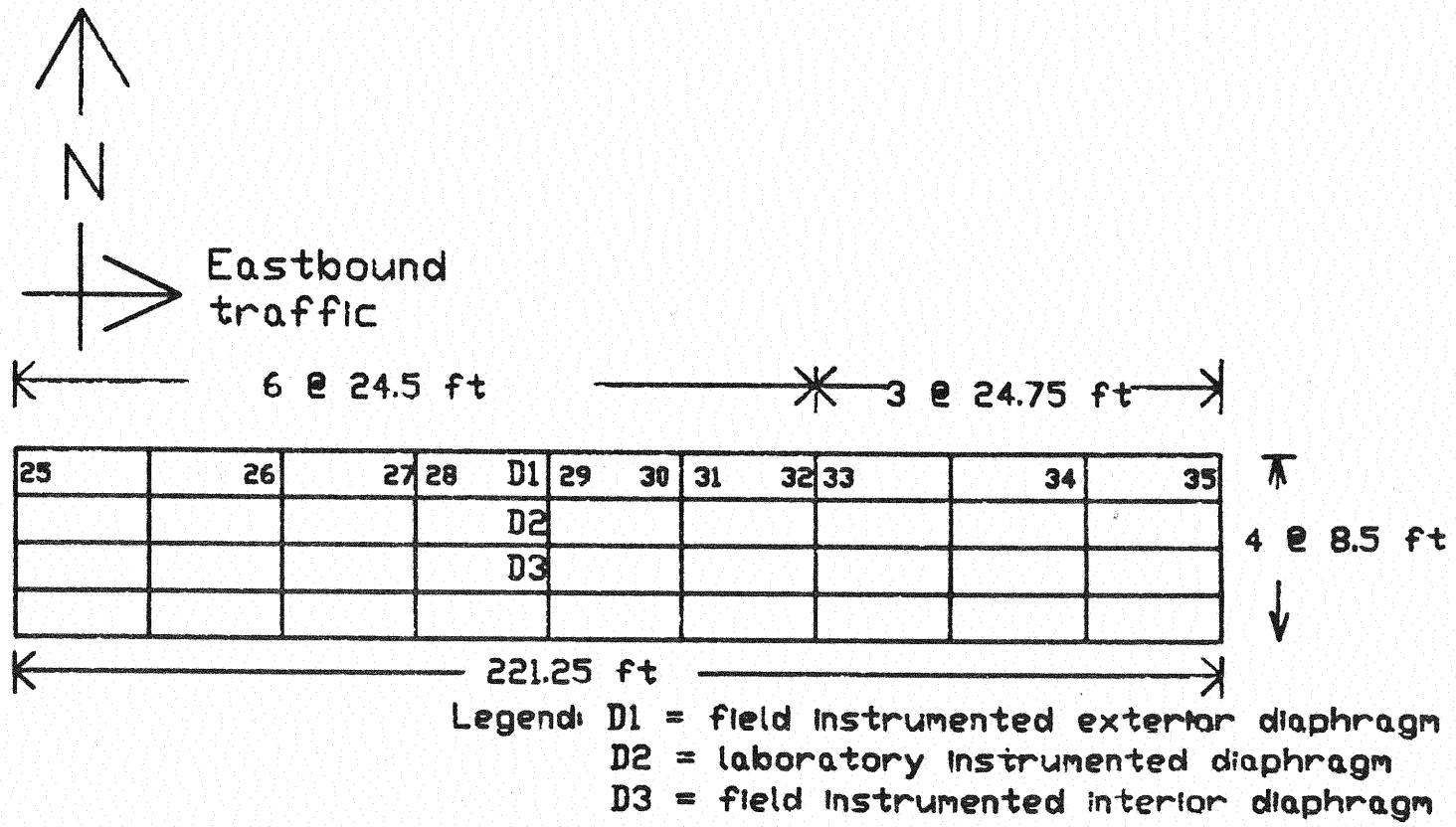

Figure 11. Shoulder Loadings at Various Positions Along First Three Spans of Bridge

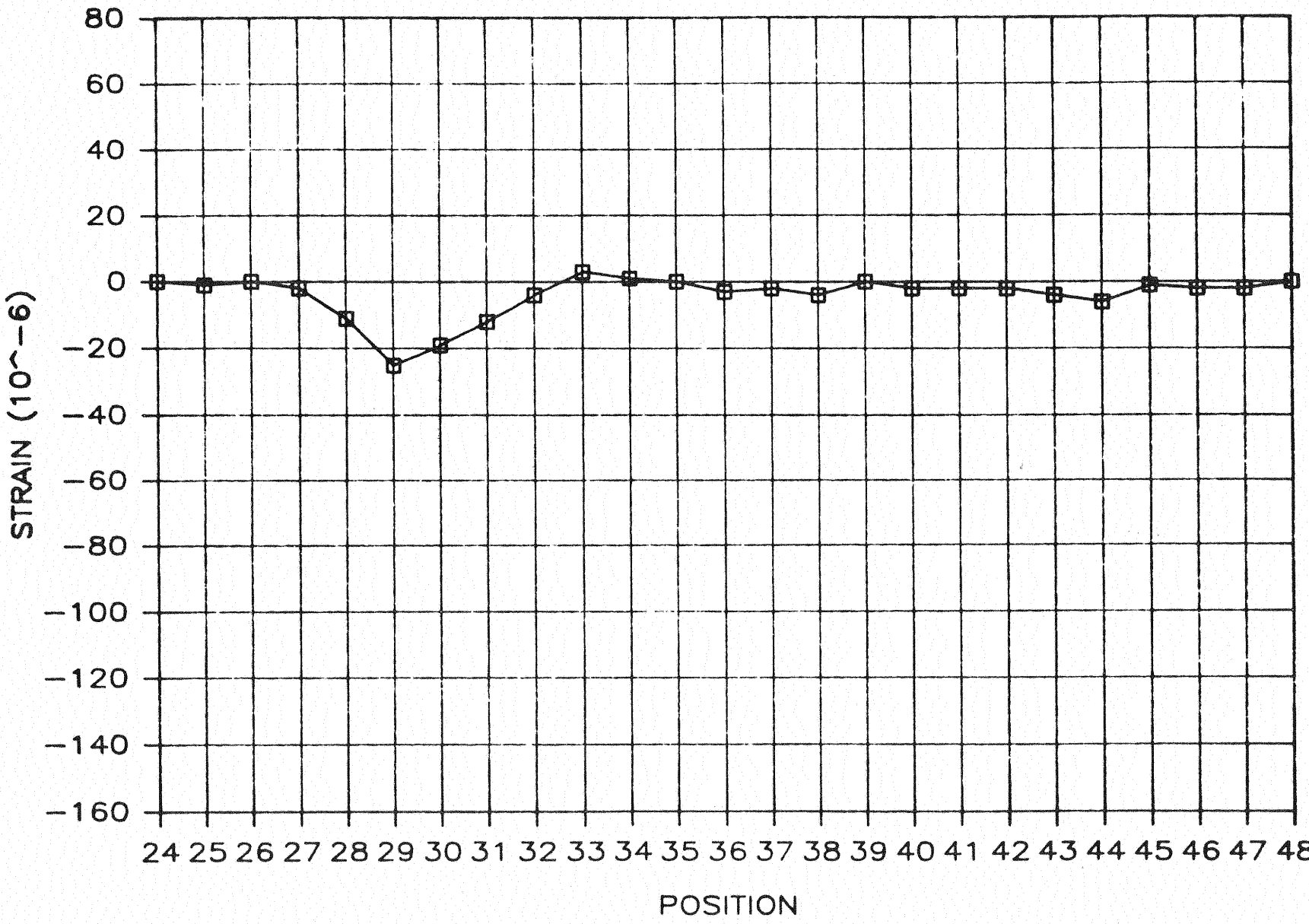

Figure 12. Strain Versus Position of Truck for Gage 22 on Laboratory Instrumented Diaphragm, Shoulder Loading

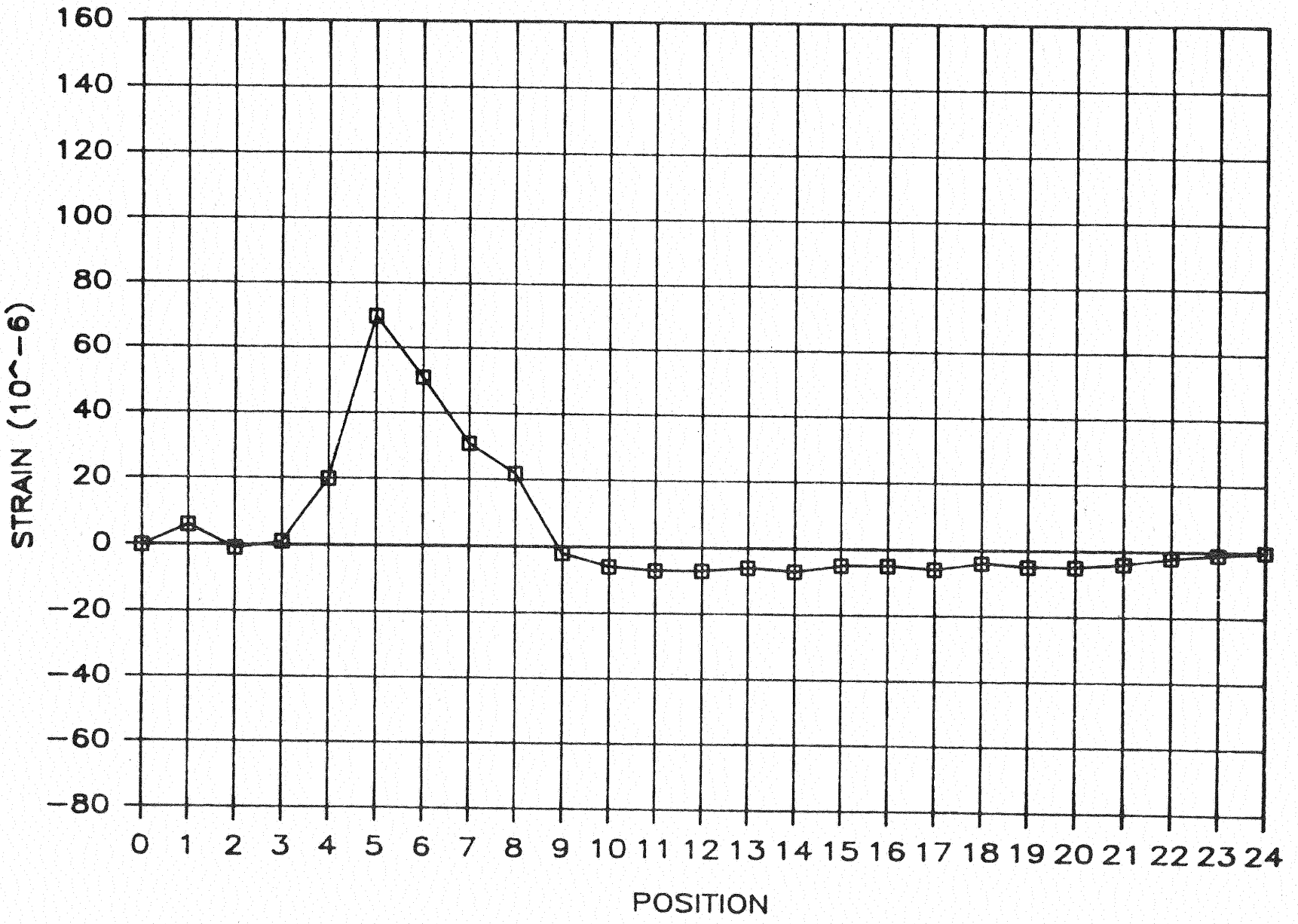

Figure 13. Strain Versus Position of Truck for Gage 8 on Field Instrumented Exterior Diaphragm, Lane Loading

ders are continuous across these three spans. In most cases, measured strains are low even when the truck is on the instrumented span. Except for obvious cases of signal noise (indicated by very abrupt and inconsistent fluctuations in measured strains), measured strains never exceed 150×10^{-6} in./in. This maximum strain was measured at gage 7 on diaphragm D1 under the lane loading condition while the rear wheels of the truck were directly over the instrumented diaphragms. Strains characteristically peak when the truck is directly over the instrumented diaphragms and the peaks tend to be in the 30×10^{-6} to 90×10^{-6} in./in. range. The strain magnitude measured on this bridge is typical of measurements made by researchers at other sites [2, 6].

Figure 14 is a plot of strain versus time for gage 8 on diaphragm D2 recorded on an x-y recorder as the tank truck moved across the bridge. The exact position of the truck at the time of peak strain was not recorded, but the shape of the curve is similar to the curves in Figures 12 and 13. There is a slight tendency for the peak strain to increase as velocity increases. Similar behavior has been observed by other researchers [7].

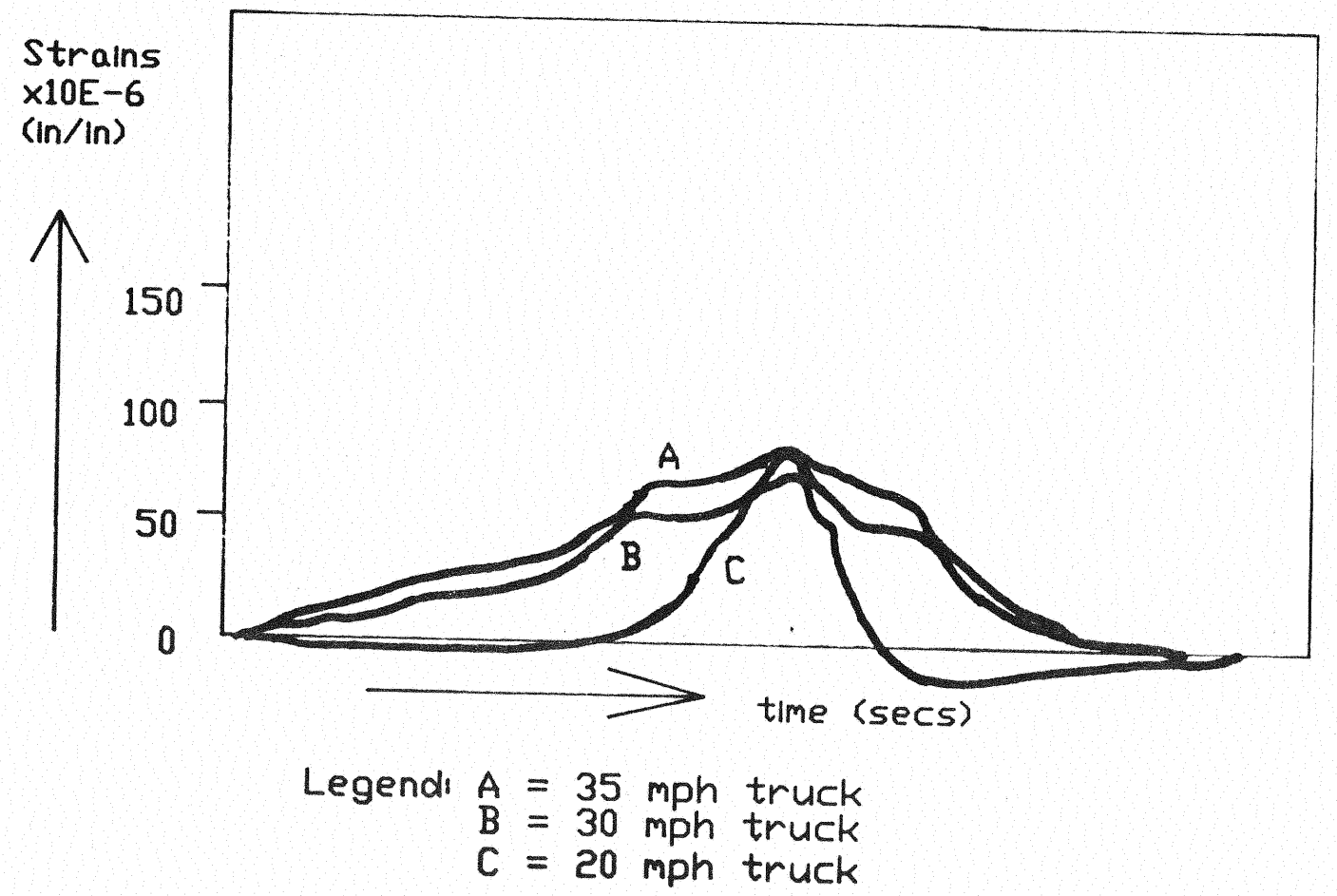

Figure 14. Strain Versus Time for Different Truck Speeds

CHAPTER 3

ANALYSIS

This portion of the investigation deals with the development of analytical models for the bridge and individual diaphragms. These models were built using STRUDL [5] on a main-frame computer. The models were built so as to match as closely as possible field conditions.

3.1 Grid Analysis of Superstructure

The final model that was adopted for the bridge superstructure was that of a grid with full composite action between the slab and the girders and diaphragms. Simple supports were assumed at the piers. Grid geometry and assumed support conditions are shown in Figure 15. This type of model has been shown to provide results comparable to more sophisticated models which treat the slab as a flat plate or as a mesh of plate elements [8].

Representative plots of measured and calculated strains versus position of truck are provided in Figures 16 and 17. Strains were calculated using simple beam theory with moments from the grid analysis. Figure 16 shows the values obtained at gage 22 for diaphragm D2 when the vehicle is located at various positions on the shoulder of the roadway. Figure 17 is a plot for gage 8 on diaphragm D1 under lane loading conditions. The strong similarity in graph shapes between the measured and calculated plots indicates that the model used is a good representation of the bridge.

3.2 Finite Element Analysis of Diaphragm

The individual diaphragm is modeled as shown in Figures 18 and 19. Eight-noded isoparametric elements are used in the web and plane truss elements are used for both flanges. The full depth of the diaphragm is

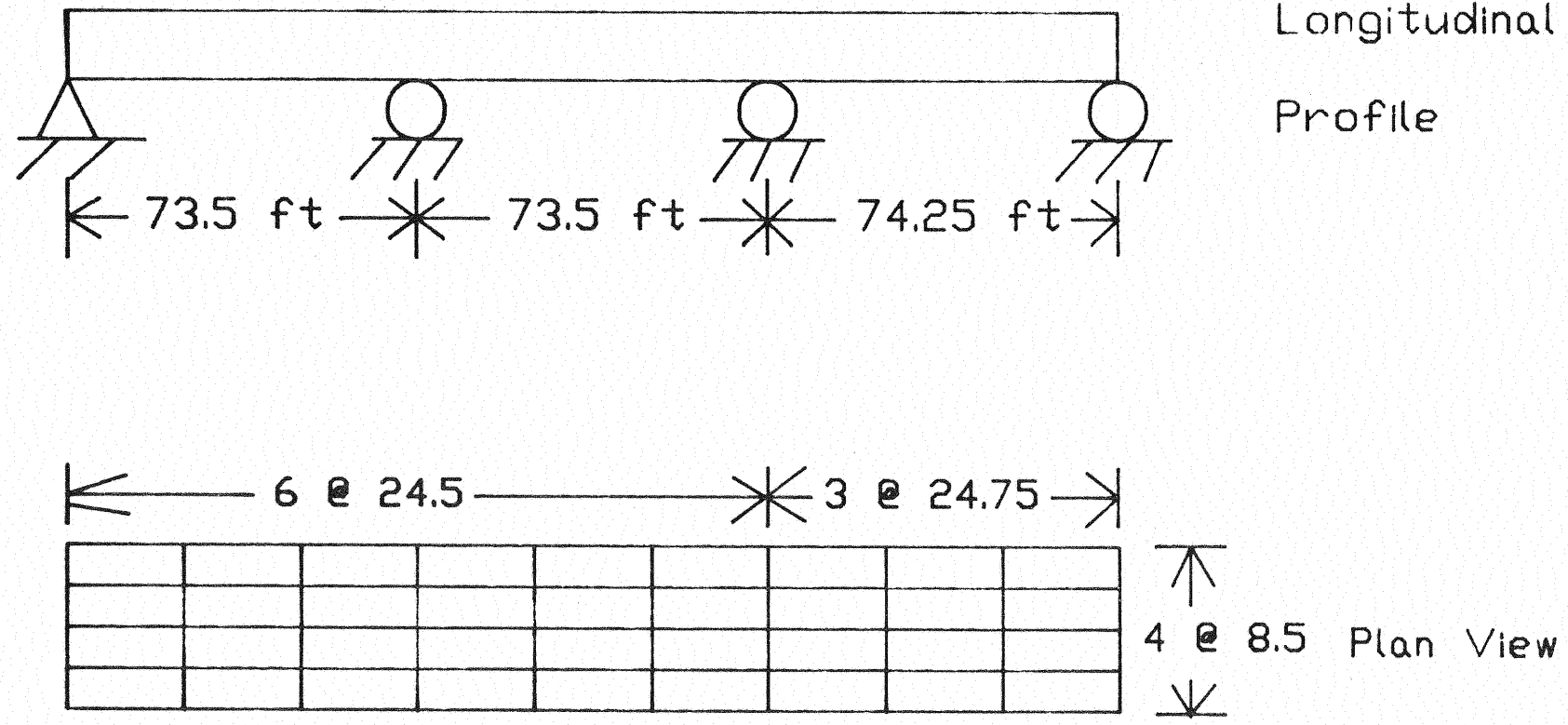

Figure 15. Grid Model of First Three Spans of Bridge

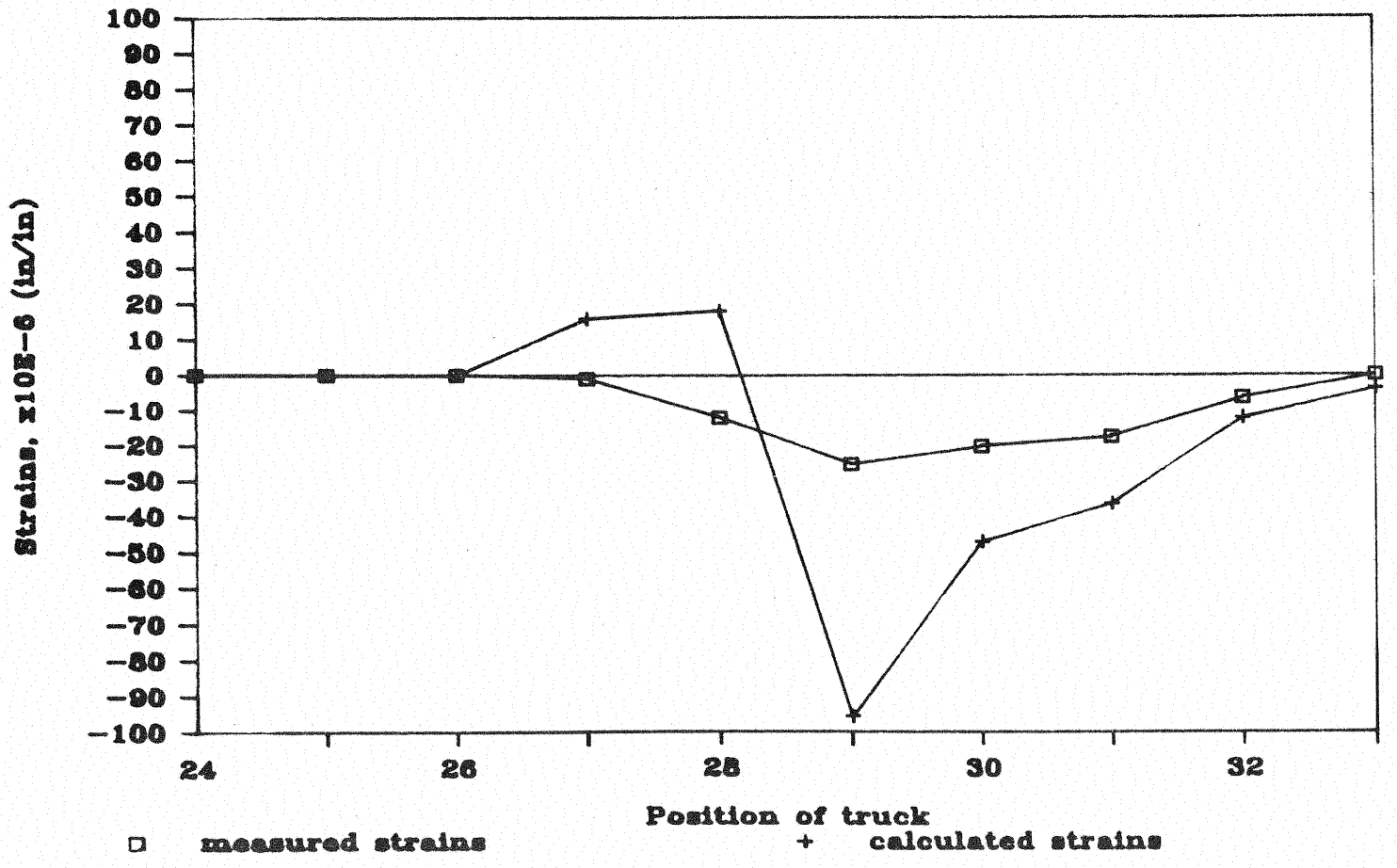

Figure 16. Comparison of Measured and Calculated Strains for Shoulder Loading, Laboratory Instrumented Diaphragm, Gage 22

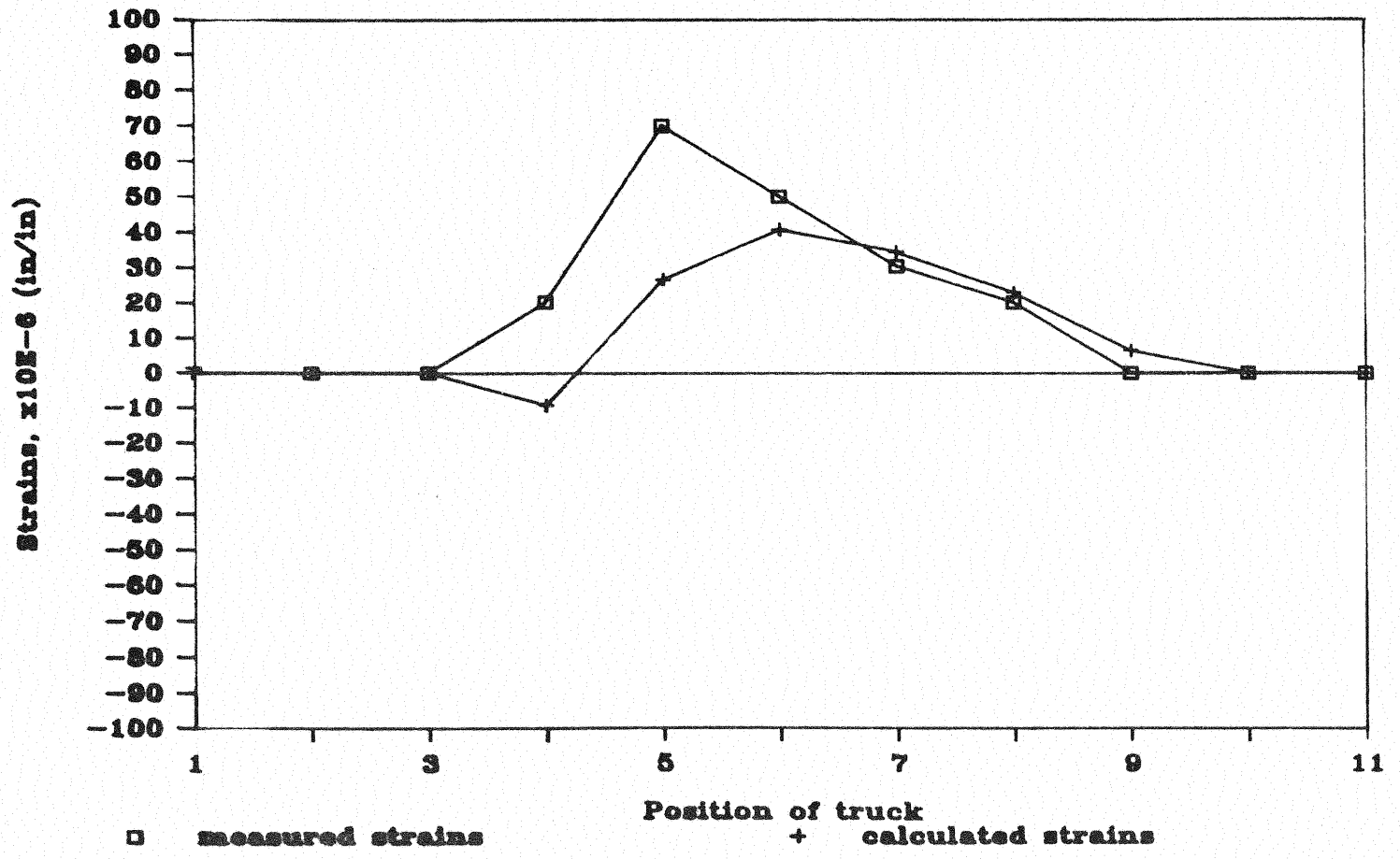

Figure 17. Comparison of Measured and Calculated Strains for Lane Loading, Field Instrumented Exterior Diaphragm, Gage 8

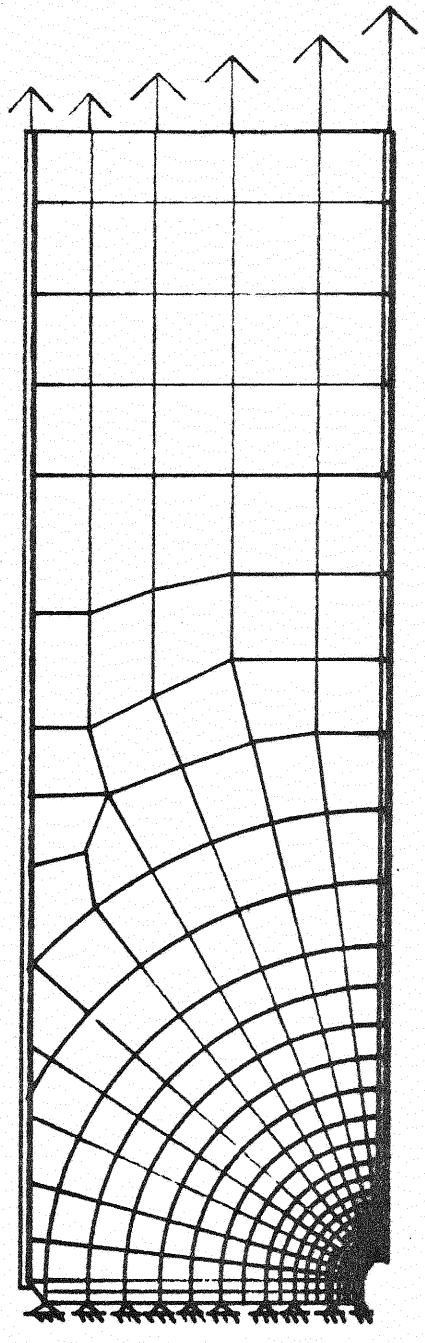

Figure 18. Finite Element Model for Diaphragm With Coped Bottom Flange

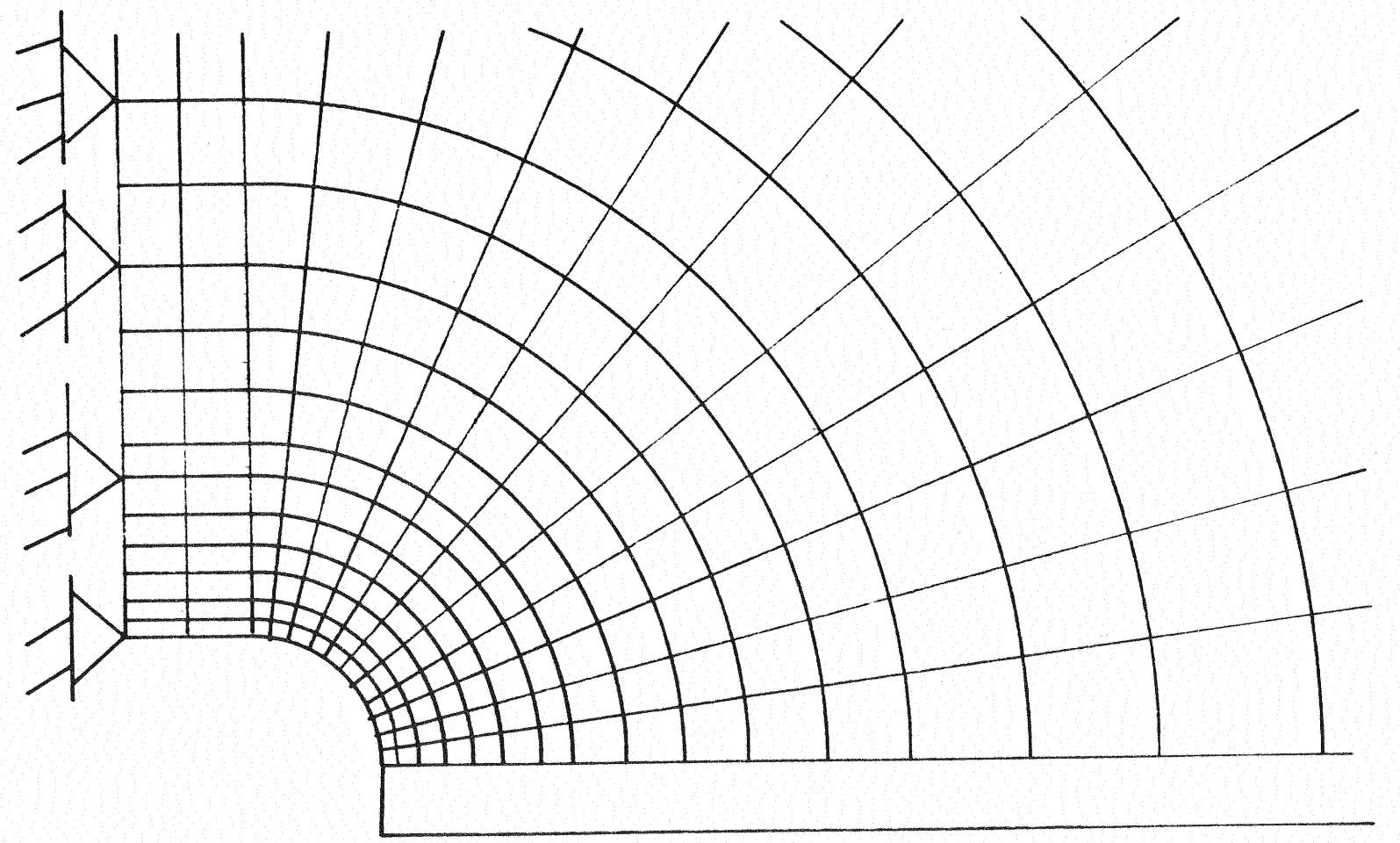

Figure 19. Magnified View of the Finite Element Model Near the Coped Flange

included in the model; the length of the model is set at three times the depth to avoid unwarranted end effects at the cope. Nodes at the left end along the bolt line are pinned to provide support. Loads applied to the right end of the diaphragm produce the stress gradient that would be present if a moment was applied to a diaphragm fully composite with a concrete deck.

The magnitude of the moment applied to the model diaphragm is ten times that obtained from the analysis of the bridge using the grid model. This is done because when the small moments obtained from the grid analysis were used, roundoff error was high. A significant error was observed between nodal stresses for elements meeting at a node. Since the emphasis in this portion of the work is to find the stress distribution along the observed crack line in the fractured diaphragm, the simplest solution is to increase the applied moment. This same moment is applied to the modified diaphragms so that changes in the stress distribution due to the modifications can be studied.

Three modified diaphragms were analyzed for comparison to the original diaphragm. The first modification does not have a bottom flange cope (Figure 20), the second modification has a cope tapered at a rate of 2.5 horizontal to 1 vertical (Figure 21), and the third modification calls for removing the bolts from the lower half of the diaphragm-to-girder connection. The degree of taper selected for the second modification is the same as that specified for flange transitions in the AASHTO Standard Specifications for Highway Bridges. The third modification was accomplished analytically by removing the pin supports from the bottom half of the connection. The first modification will require replacing the diaphragms while the second and third modifications can be applied to existing diaphragms.

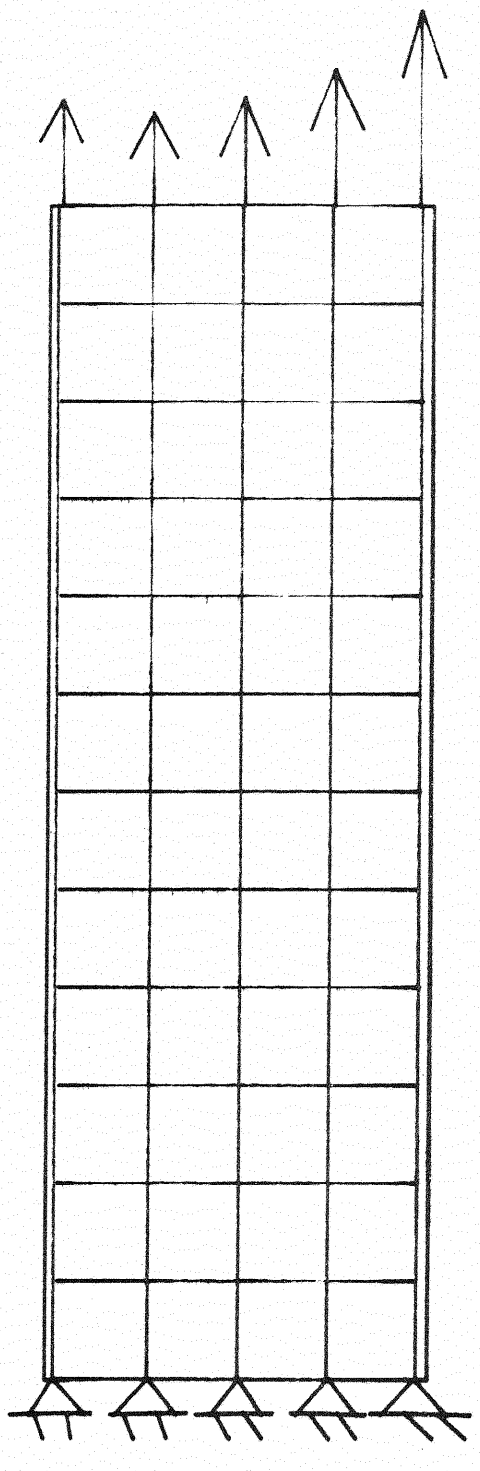

Figure 20. Uncoped Diaphragm

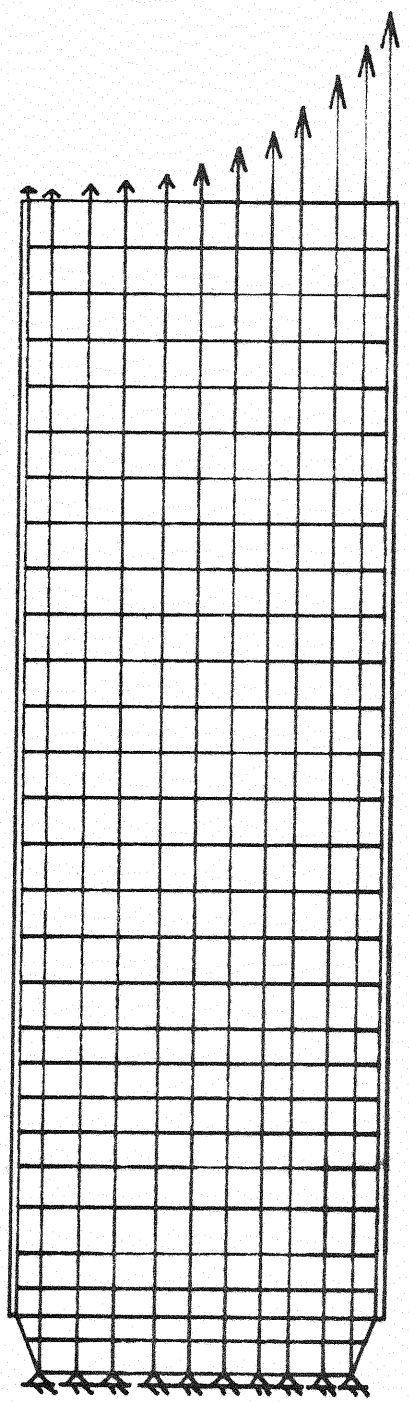

Figure 21. Diaphragm With Tapered Cope

Stresses calculated along the crack line for the four analytical models are shown in Figure 22. In examining this figure, recall that the moments applied to the models are ten times greater than the moments calculated from the grid analysis. Also recognize that the analysis is an elastic analysis; calculated stresses are not restricted by a plastic limit. The sole purpose of this figure is to show how the stress distribution in the vicinity of the cope changes as diaphragm modifications are applied.

As seen in Figure 22, all modifications succeed in reducing stress at the cope. The tapered cope provides only a slight reduction while the uncoped diaphragm and the diaphragm with bolts removed from the connection provide significant reductions. Removing the cope from the bottom flange leads to a relatively uniform stress distribution, while removing bolts from the bottom of the connection causes the peak stress to shift up away from the cope.

The results of the analyses indicate that the most effective way of reducing stress in the diaphragm at the connection is to install an uncoped diaphragm. In the uncoped diaphragm, there are no points of high stress concentration. Removing bolts from the bottom half of the diaphragm-to-girder connection is also effective in reducing stress at the cope, but results in a high stress in the center portion of the web. Tapering the cope reduces stress at the bottom of the diaphragm, but to a much lesser degree than the other two modifications.

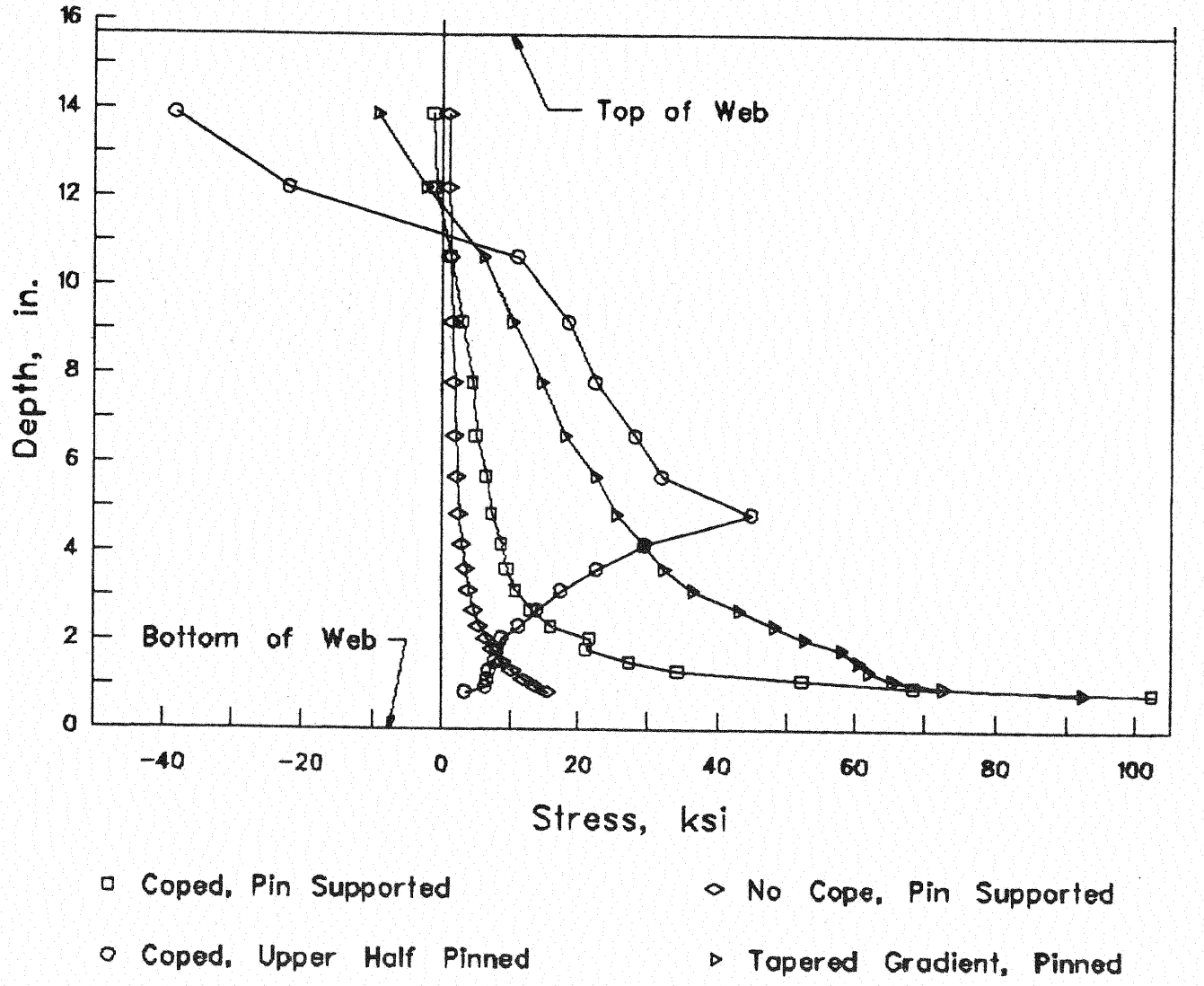

Figure 22. Stress Along Crack Line From Finite Element Analysis

CHAPTER 4

LABORATORY TESTING

4.1 Physical and Chemical Properties

Notes on the structural drawings of the subject bridge show that the steel in the bridge is required to satisfy American Society for Testing and Materials (ASTM) Standard A36. A chemical analysis of diaphragm flange material has confirmed that the composition of the steel falls within tolerance limits set out in ASTM A36. Tension tests performed in accordance with ASTM E8 using rectangular tension test specimens also confirm that the material falls within the A36 Standard. Results from the chemical analysis and the tension tests are tabulated in Appendix A. Charpy impact tests were performed in accordance with ASTM A370 using standard thickness specimens from the flange and reduced thickness specimens from the web. Test results show that the steel provides substantially more impact resistance than the 15 ft lbs at 40°F required by AASHTO for bridges in Oklahoma. Plots of the Charpy data are provided in Figures 40 and 41 of Appendix A. There are no unusual physical or chemical properties in the diaphragm steel which would contribute to the cracking problem.

4.2 Fatigue Tests

The original detail and four different modifications were tested under cyclic load in the laboratory. Support conditions and loading were configured to match field conditions as closely as possible. The modifications tested include: (1) no cope in bottom flange, (2) tapered cope, (3) bolts removed from the bottom two bolt holes, and (4) adding an auxiliary flange. The original detail is shown in Figure 23, the tapered cope is shown in

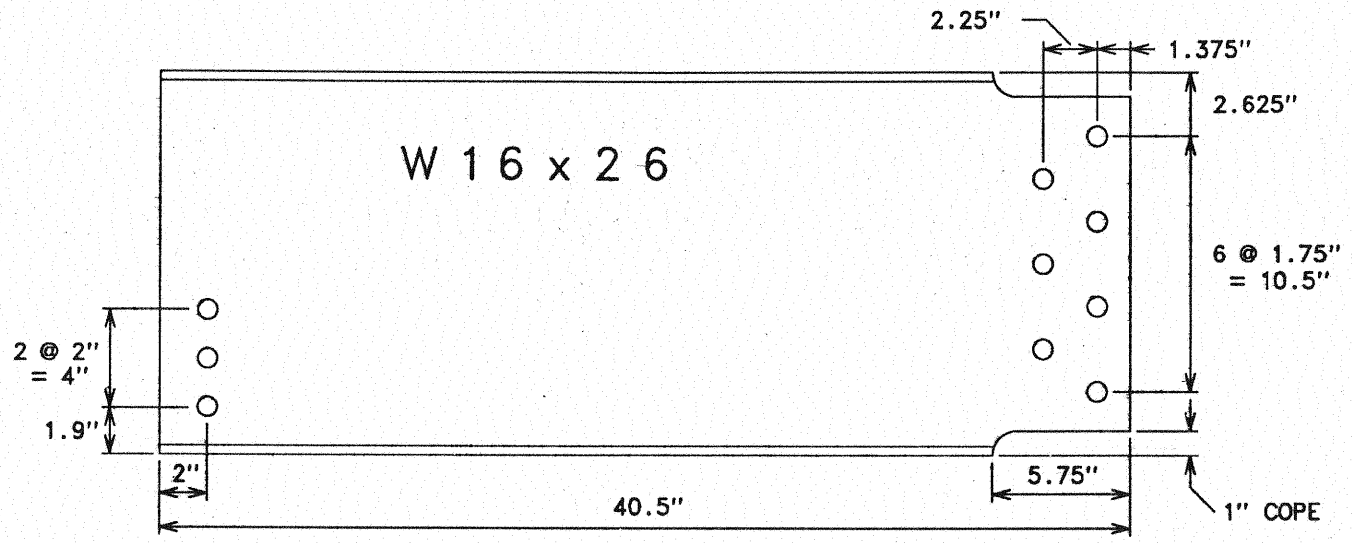

Figure 23. Test Specimen for Original Detail

Figure 24, and the auxiliary flange is shown in Figure 25. The first three modifications were evaluated with a finite element analysis prior to testing. The fourth modification was added after the start of the fatigue testing program. All modifications will be evaluated on the basis of their ability to increase fatigue life beyond that measured for the original detail.

4.2.1 Apparatus

Loads were applied using a closed-loop servo-hydraulic system. The test frame and control system are shown in Figure 26. The test frame consists of two short vertical members with a horizontal member connecting the tops of the verticals. The verticals provide support for the ram and specimen and transfer the test load into the reaction floor. The horizontal member adds rigidity to the system, provides upward support for the ram and specimen, and is used to help prevent lateral displacements of the specimen.

The test specimens are the deeper wide flange members seen below the top horizontal member in Figure 26. The specimen on the right is connected at its right end to the vertical. On its left end the specimen is bolted to a gusset plate simulating the connection on the bridge. The gusset plate is welded to a tee-shaped section simulating the longitudinal bridge girder. A photograph of the simulated girder and connections is provided in Figure 27. Another specimen is bolted to the left side of the simulated girder and then attached at its left end to the hydraulic actuator. This arrangement models the relevant portion of the actual connection and allows two specimens to be tested simultaneously.

To produce the stress distribution that would be present in a composite beam loaded in bending, without actually constructing a composite beam, it

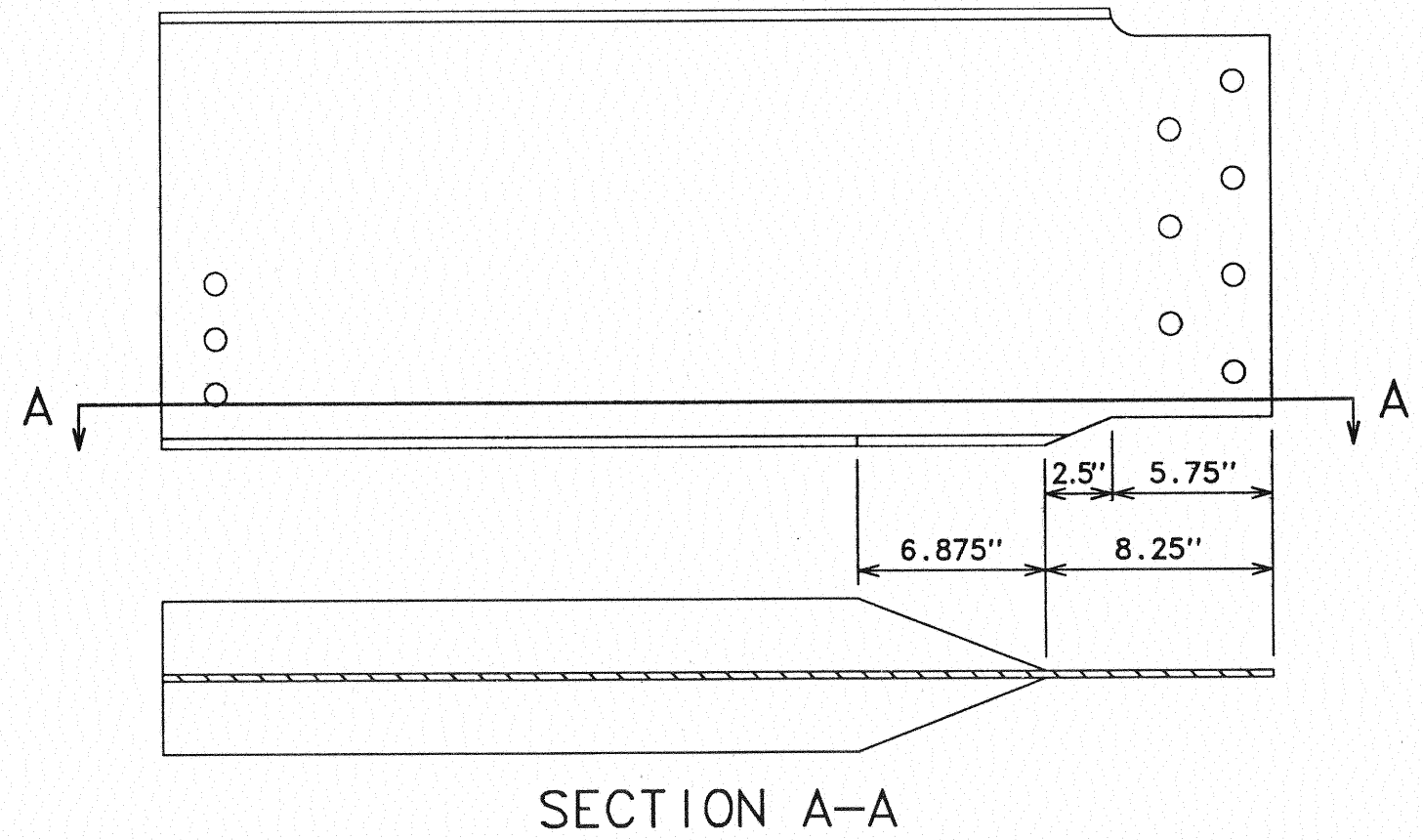

Figure 24. Tapered Cope Detail

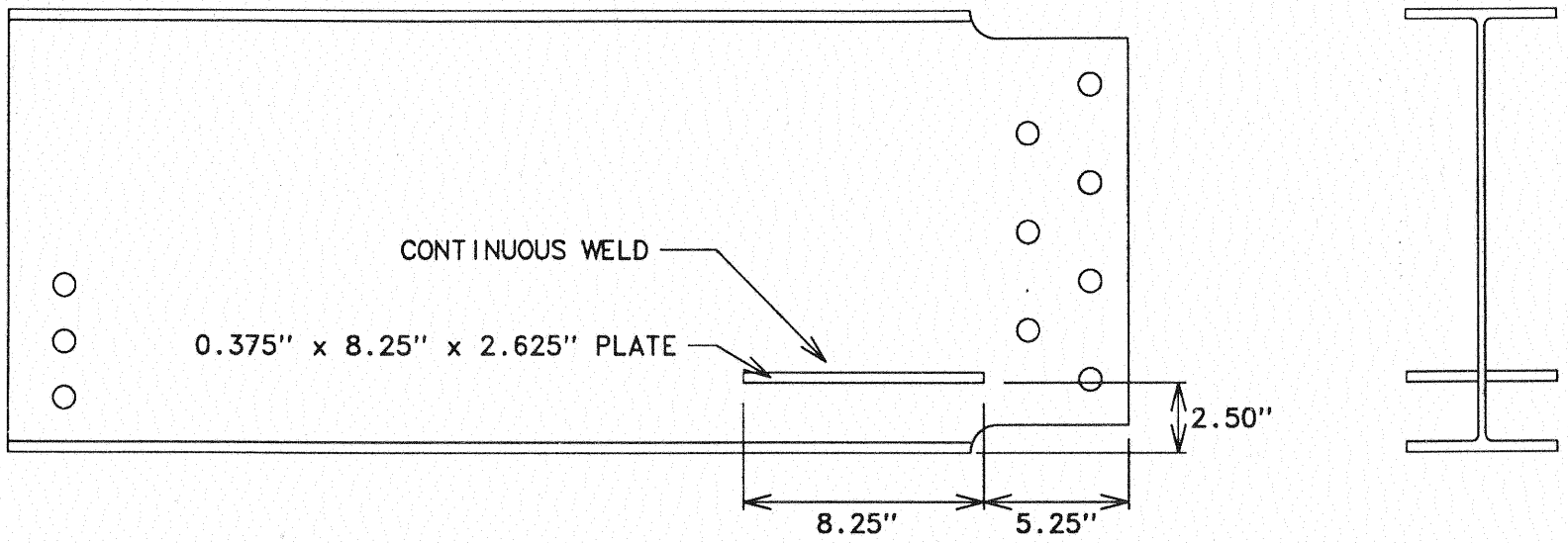

Figure 25. Auxiliary Flange Detail

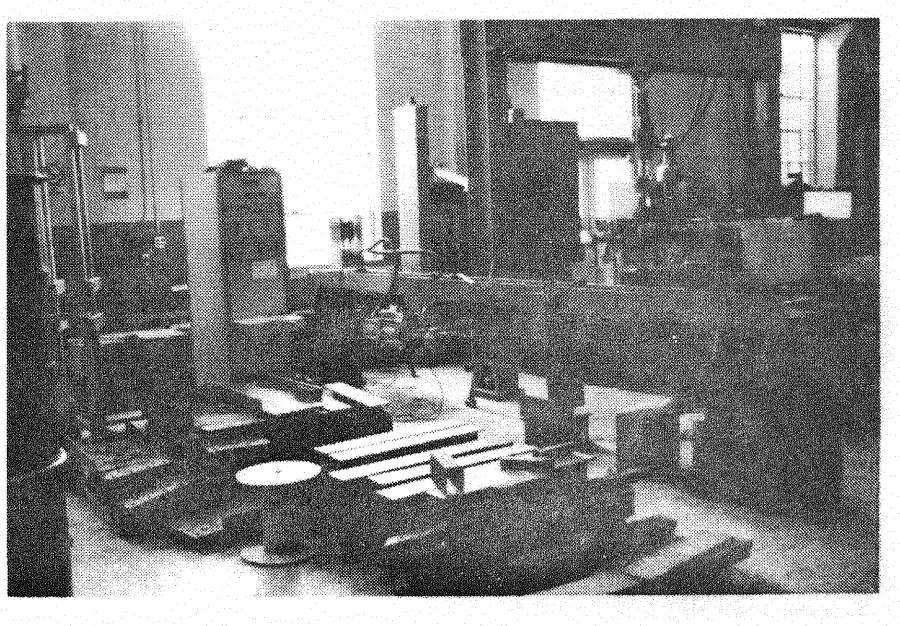

Figure 26. Testing Equipment

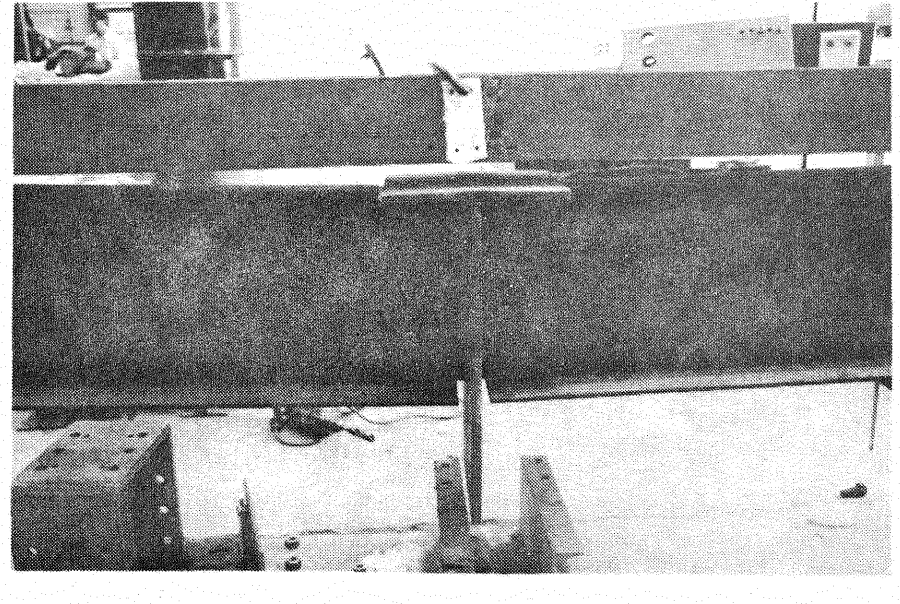

Figure 27. Simulated Girder

was necessary to apply an eccentric axial load to test specimens. This eccentricity was achieved in the tests by positioning the diaphragm-to-column connection and the diaphragm-to-actuator connection below the diaphragm centerline. The three bolt holes at the left end of the specimens shown in Figures 23, 24, and 25 are vertically offset from the diaphragm centerline to provide the required eccentricity. Connections to the vertical supports and to the actuator were made with pins so that no additional moment above that produced by the eccentric load would be introduced at these connections.

To restrict movement transverse to the test specimens at the simulated girder, it was necessary to restrain the girder in its longitudinal direction. In the bridge, this restraint would be provided by the attachment of the girder to the deck. The restraints, which are shown in Figure 28, bolt to the girder in three locations: the upper web on both ends of the girder and the lower web on one end of the girder. Each restraint uses two Teflon pads which are able to slide freely against each other in the direction longitudinal to the diaphragms, but are blocked from moving transverse to the diaphragms.

4.2.2 Results

All specimens were tested under a load-time history which varied sinusoidally with time at a constant amplitude. Load range varied between tests, but the ratio of minimum to maximum load (load ratio) was held constant. Loads used in tests and the corresponding nominal stress ranges at the cope are shown in Table 1. Nominal stress ranges are calculated assuming simple beam theory.

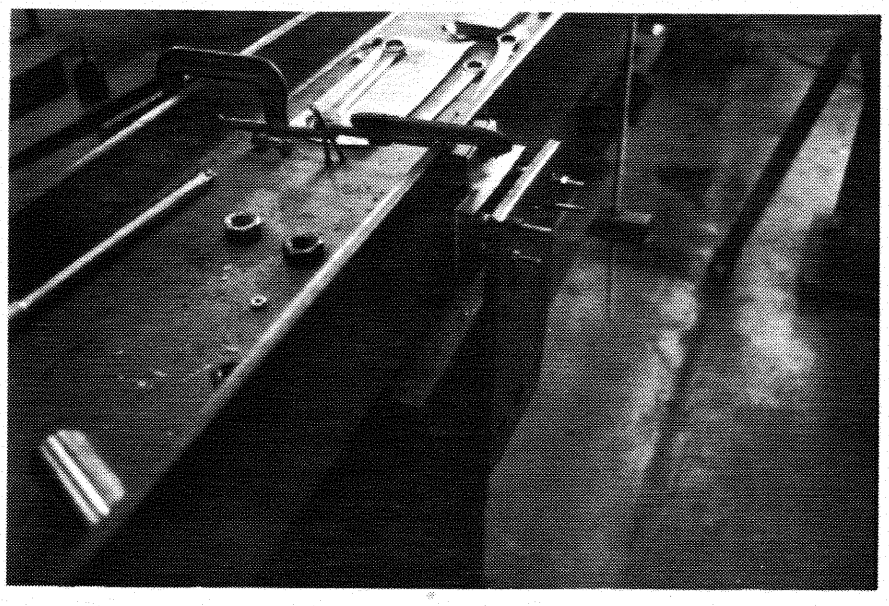

(a) Top

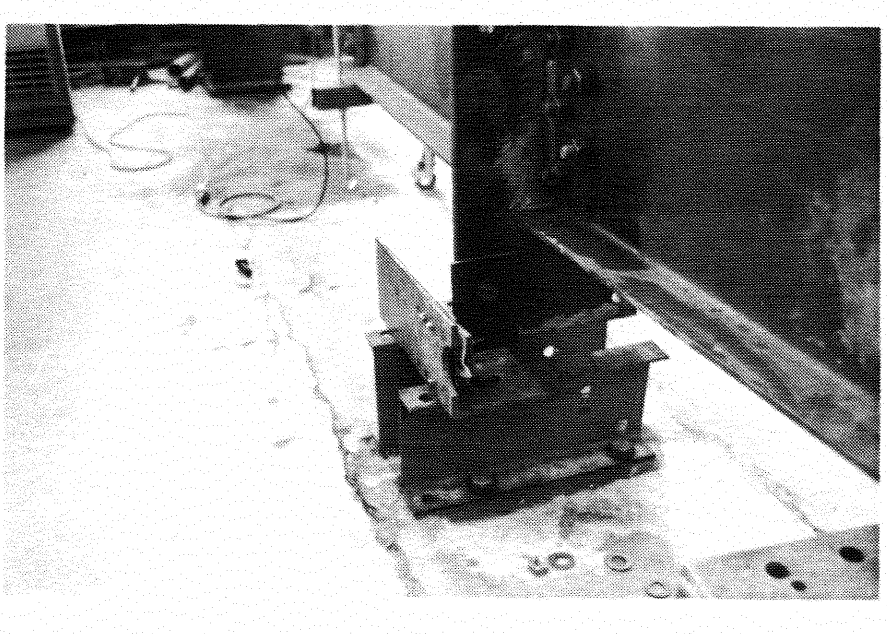

(b) Bottom

Figure 28. Lateral Restraints

TABLE 1

APPLIED LOADS AND NOMINAL STRESS RANGES

Load, Kips Max.	Min.	Load Range, Kips	Nominal Stress Range, KSI
29.4	4.4	25	20
23.5	3.5	20	16
17.7	2.7	15	12
11.8	1.8	10	8

Stresses applied to the diaphragm in the laboratory are much greater than those measured in the field. Higher stresses were used in the laboratory to reduce testing time. This does not detract from the capacity of the tests to satisfy their primary purpose, which is to demonstrate the effectiveness of the modifications at increasing fatigue life relative to the original detail.

Original Detail. The first tests were conducted on the original connection detail. To verify that the load and support systems were producing the strain gradient anticipated for a composite beam loaded in bending, the first laboratory diaphragm was instrumented with three strain rosettes as shown in Figure 29. Strains measured at gages 2, 5, and 8 for a 30-kip load are plotted in Figure 30. As expected, longitudinal strain reaches a tensile maximum at the bottom of the beam and decreases toward the top of the beam.

The rosette data were also used to determine the magnitude and direction of principal stresses at gage locations. Principal stress elements are shown in Figure 31. The important observation to be made from this figure is that the maximum tensile stress is oriented perpendicular to the anticipated crack plane.

The original detail was tested under cyclic loads at a variety of stress ranges. The data obtained are shown in Table 2, and a plot is shown in Figure 32. A line fit to the data using the least squares method is also shown on the plot. Data for tests discontinued without initiating noticeable cracks are indicated by an arrow attached to the data point and are not included in the regression analysis. The 90% confidence limit lines shown on the plot indicate there is a 90% probability that future values would fall within the limits. The detail can be placed in a specific stress

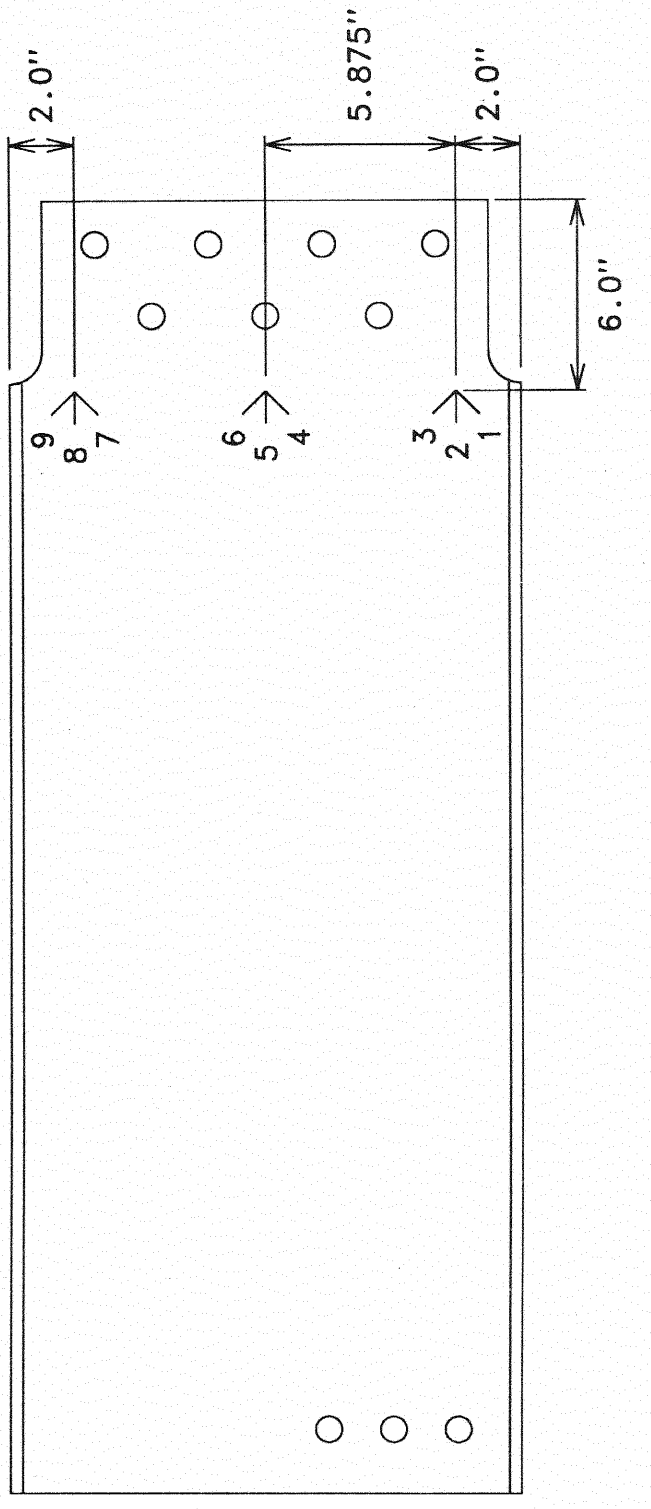

Figure 29. Position of Strain Rosettes

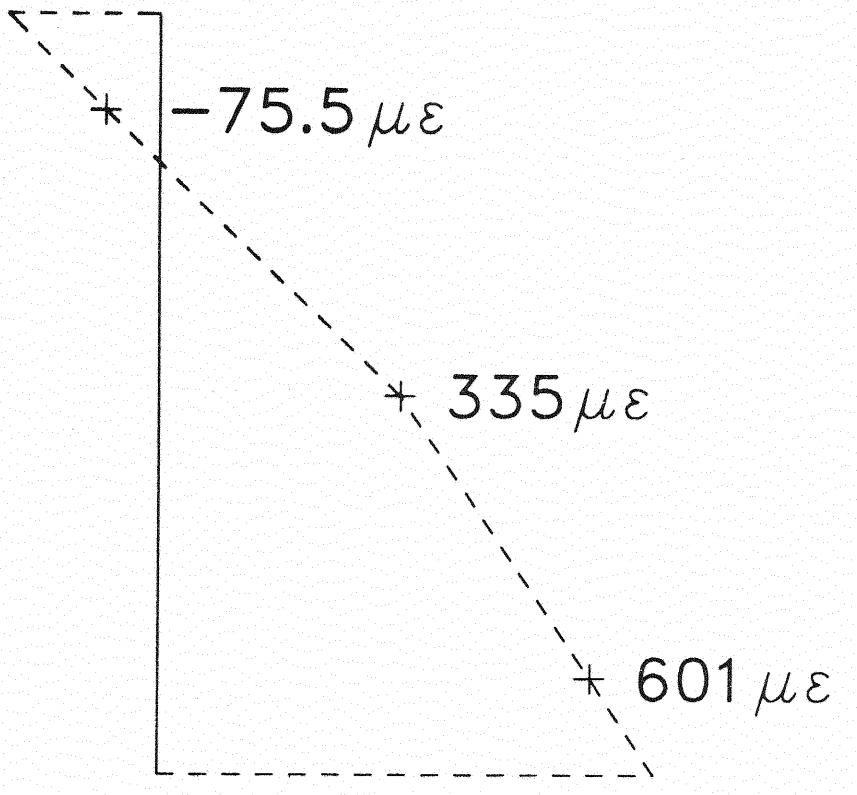

Figure 30. Distribution of Horizontal Strains

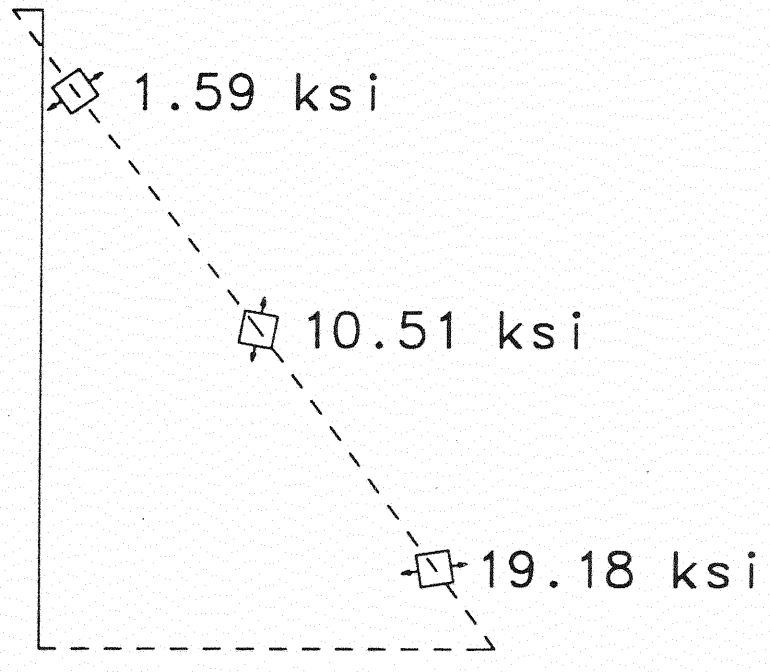

Figure 31. Principal Stresses Near Cope

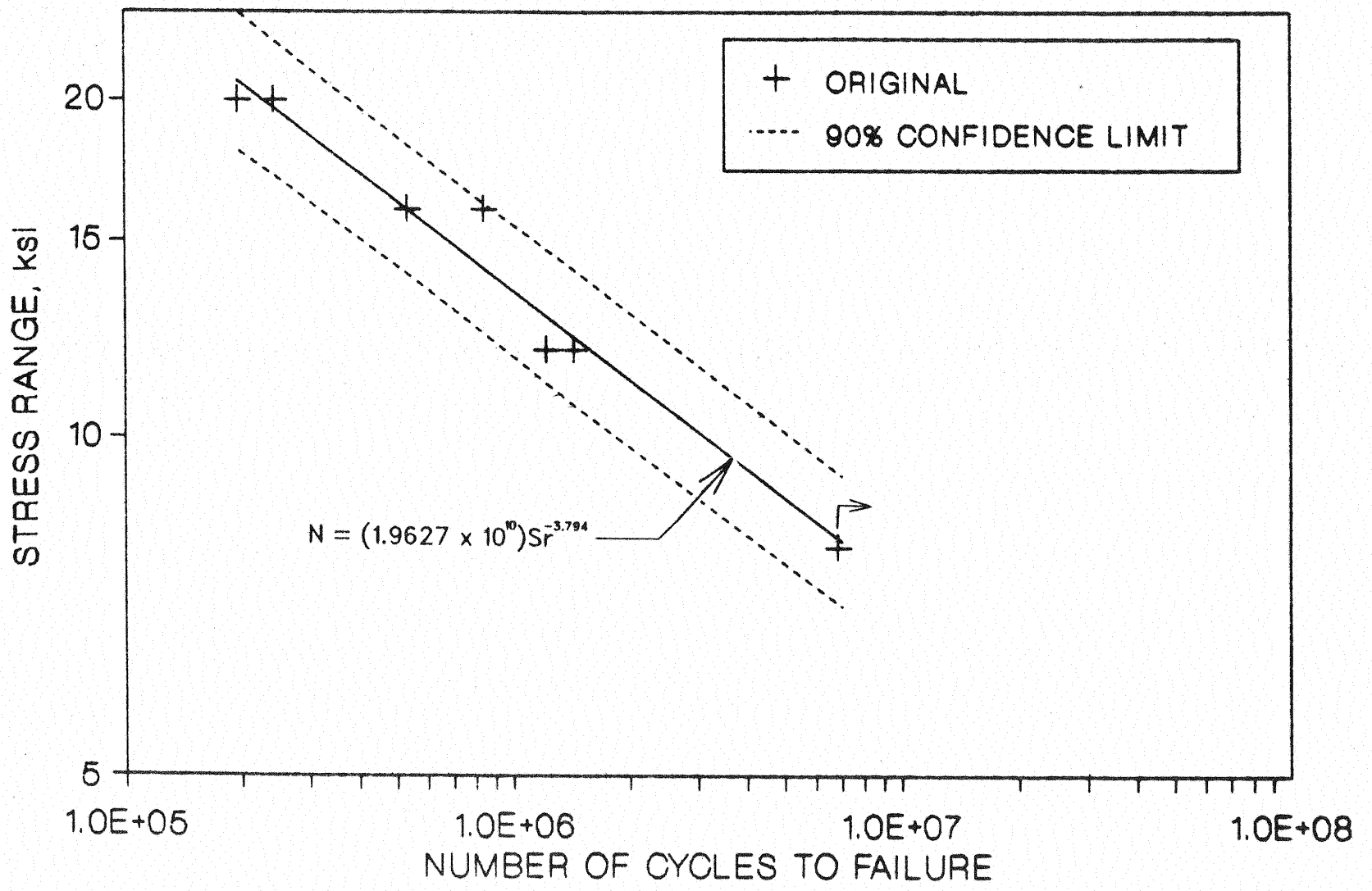

Figure 32. Fatigue Life of Original Detail

TABLE 2

FATIGUE LIFE OF ORIGINAL DETAIL

Stress Range, KSI	Number of Cycles to Failure
20	195160
	240740
16	529660
	835220
12	1213240
	1431580
8	6824790*
	6824790*

*Tests were discontinued.

category as discussed in Reference [3]. The fatigue data are replotted in Figure 33 with the corresponding stress category superimposed.

Failed specimens are shown in Figure 34. Specimens were considered to have failed when the crack had grown through half the web. It was found that very few cycles relative to the total number of cycles applied were necessary to propagate the crack from the web centerline through the upper half of the web. Stopping the tests when the cracks reached the web centerline was necessary to prevent the specimens from becoming so flexible that they would impact on the load frame during cycling. An important observation to be made from Figure 34 is that the crack shape is very similar to shapes observed on the bridge and that the crack plane is approximately perpendicular to the direction of the maximum principal tensile stress shown in Figure 31.

No Cope in Bottom Flange. Two specimens were tested at the 20 ksi stress range. Data are recorded in Table 2 and plotted in Figure 35. Both specimens withstood over two million load cycles with no sign of fatigue damage. The data points plot well beyond the upper 90% confidence limit for the original detail, indicating that a significant improvement in fatigue life has been achieved.

Tapered Cope. The fatigue life of the tapered cope detail was very dependent on how carefully cutting and grinding procedures were carried out. As can be seen in Table 3 and Figure 35, the two tapered cope specimens exhibited significantly different fatigue lives. One test resulted in a substantial increase over the life of the original detail while the other resulted in only a minimal increase. A failed specimen is shown in Figure 36. Cracks in these specimens originated at rough spots on the tapered surface and grew into approximately the same shape as on the original detail.

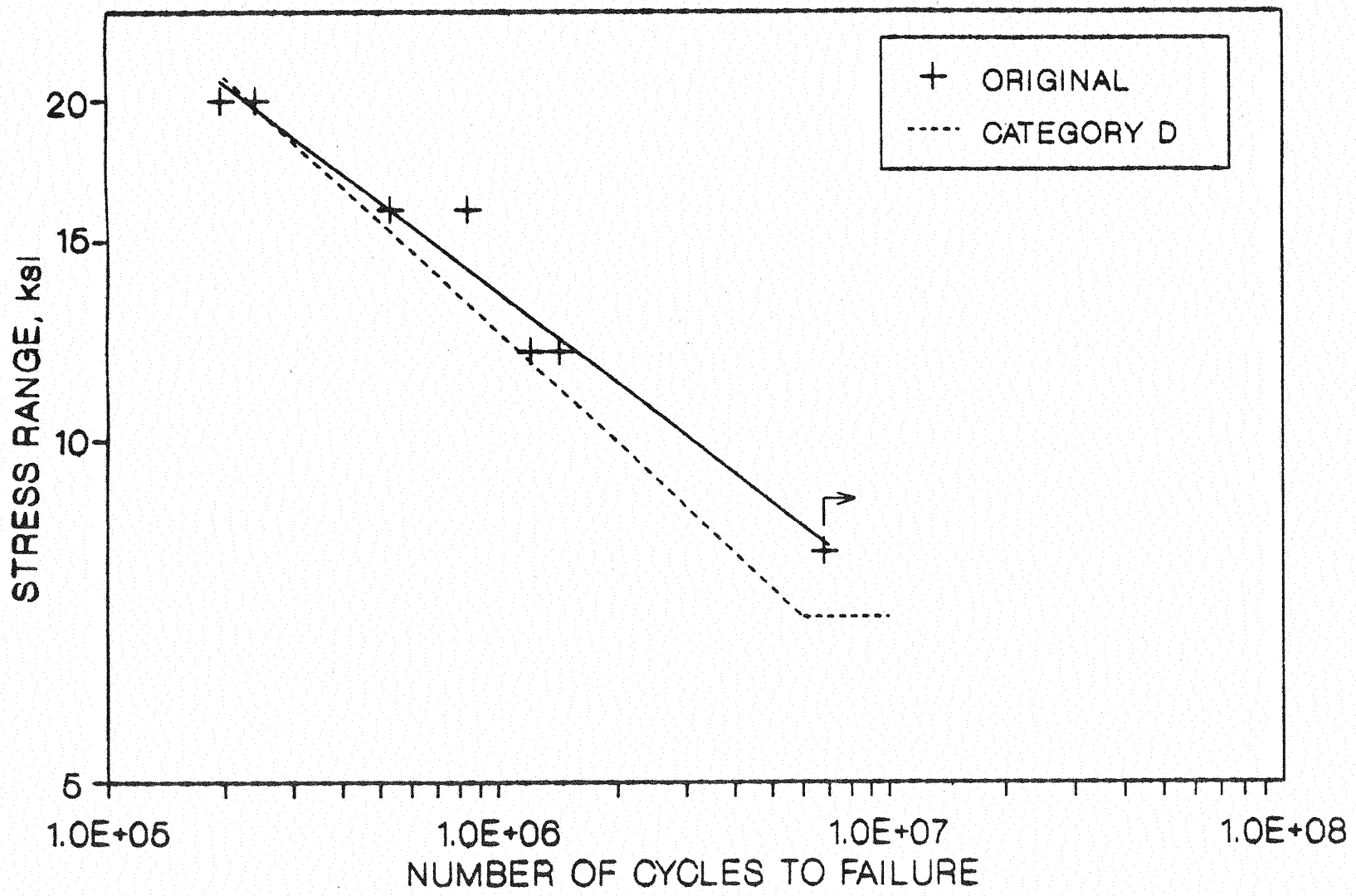

Figure 33. Fatigue Life of Original Detail Compared to a Category D Detail

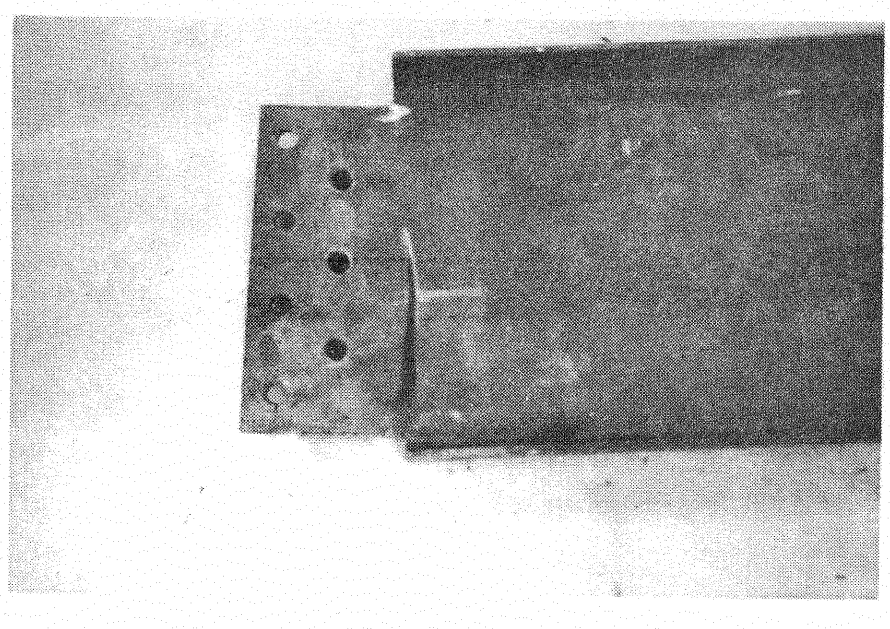

(a)

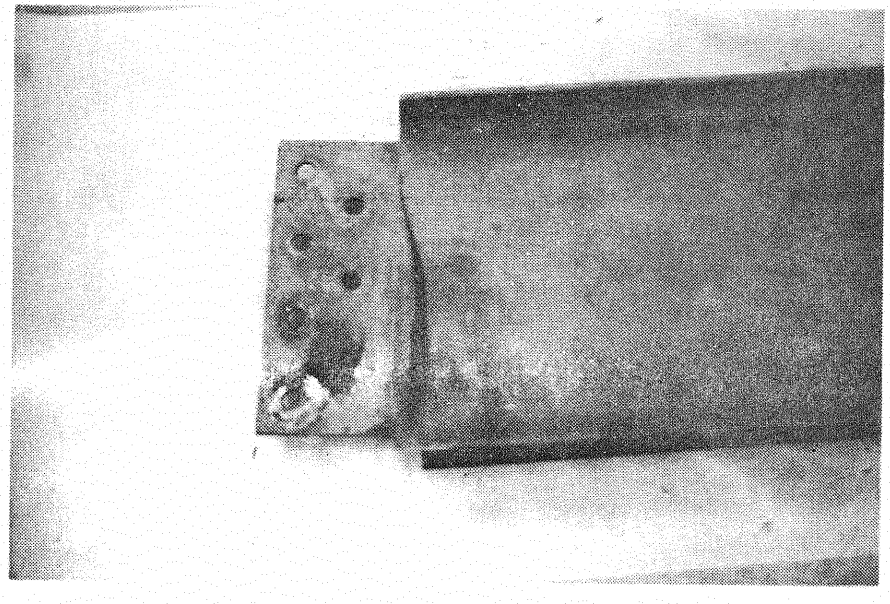

(b)

Figure 34. Typical Cracking Pattern in Laboratory Specimens

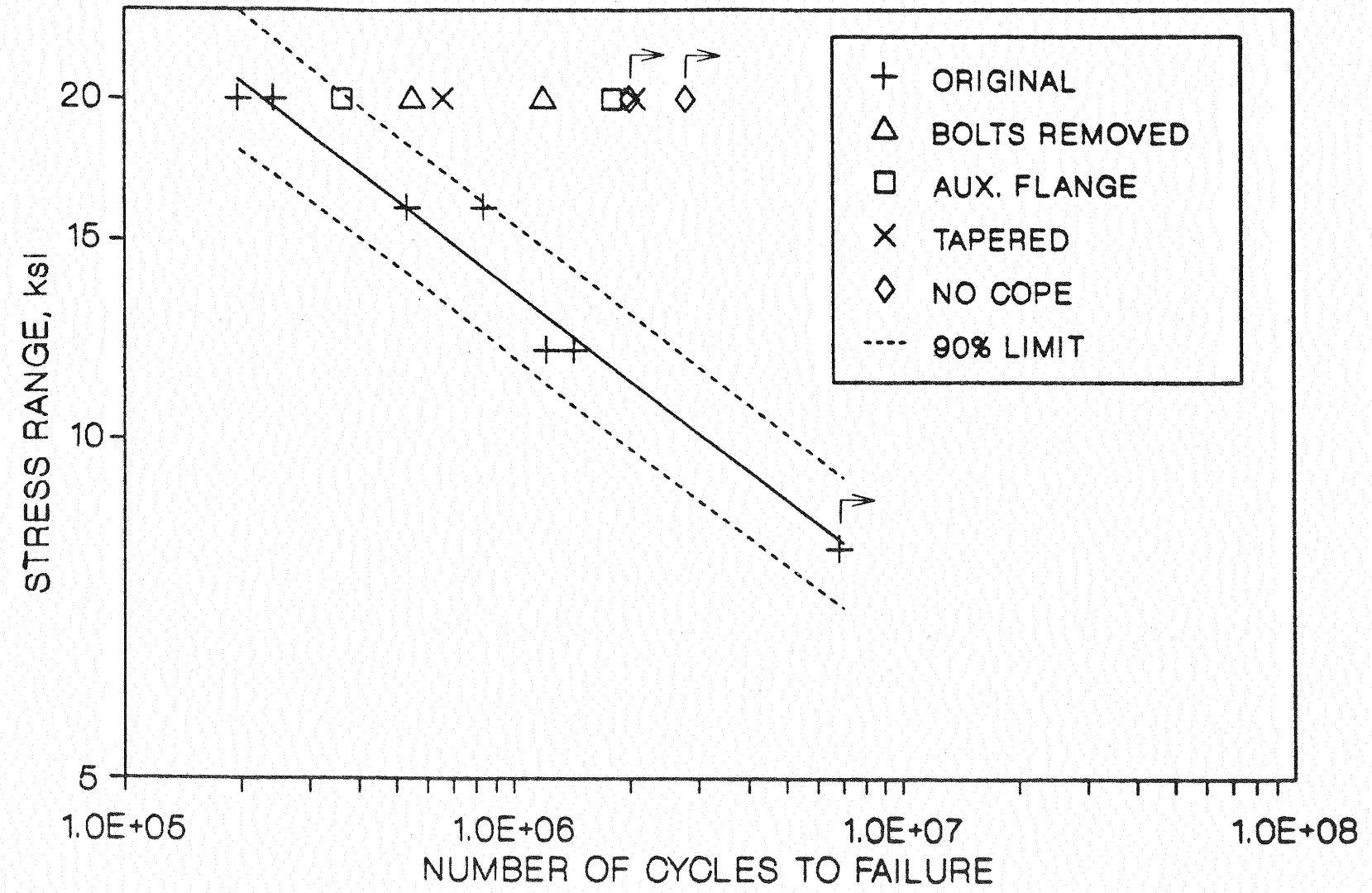

Figure 35. Fatigue Life of All Specimens

TABLE 3

FATIGUE LIFE OF MODIFICATIONS

Modification	Number of Cycles to Failure for 20 KSI Stress Range
Two lower bolts removed	1188380 547730
Auxiliary flange	360940 1790810
Tapered cope	656590 2066660
New member with no cope	2788480* 2001970*

*Tests were discontinued.

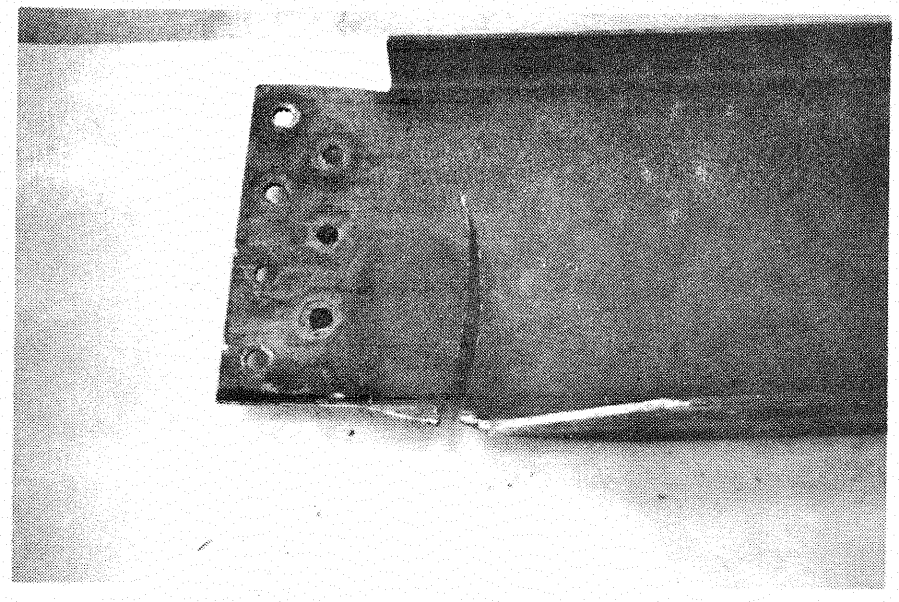

Figure 36. Failure of Tapered Cope Detail

Bottom Bolts Removed. Removal of the two lowest bolts relieves the stress at the lower cope, but still leaves the connection with sufficient capacity to carry the wheel loads of an HS20 truck. (Calculations are shown in Appendix B.) In Figure 37, the magnitude and direction of principal stresses in the diaphragm when all bolts are in place are compared to the stresses when the lowest two bolts are removed. Strains with bolts removed were measured using the same beam described in the discussion of the original detail. The shape of the measured stress distribution is in agreement with results of the finite element analysis shown in Figure 22.

Fatigue data are recorded in Table 3 and plotted in Figure 35. Data points for the two specimens tested plot beyond the upper 90% confidence limit for the original detail, indicating the modification is effective at increasing the diaphragm fatigue life. Average fatigue life for this detail is slightly less than for the tapered cope, but scatter in the tapered cope data is greater. Neither this detail nor the tapered cope is as effective at increasing fatigue life as is the uncoped detail.

Failure in these specimens resulted from a crack originating in one of the lower bolt holes and growing out to the side or bottom of the diaphragm. Photographs of failed specimens are shown in Figure 38. The observed mode of failure may be partially the result of the loading system used in all the tests. Since the eccentricity at the diaphragm-to-column and diaphragm-to-actuator connections was fixed in the tests, removal of the bottom two bolts increased the eccentricity and therefore the moment on the connection. In the bridge, the moment is caused by differential deflections of the longitudinal girders, not by an eccentrically applied load. Removal of the lowest two bolts in the connections on the bridge may actually reduce the moment in the diaphragms by making them more flexible. The five remaining bolts will

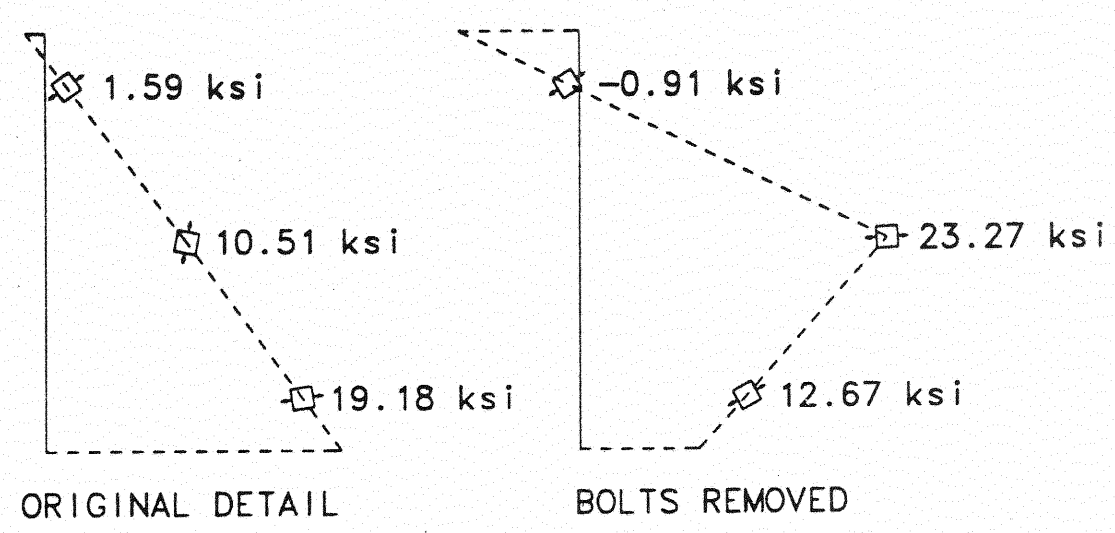

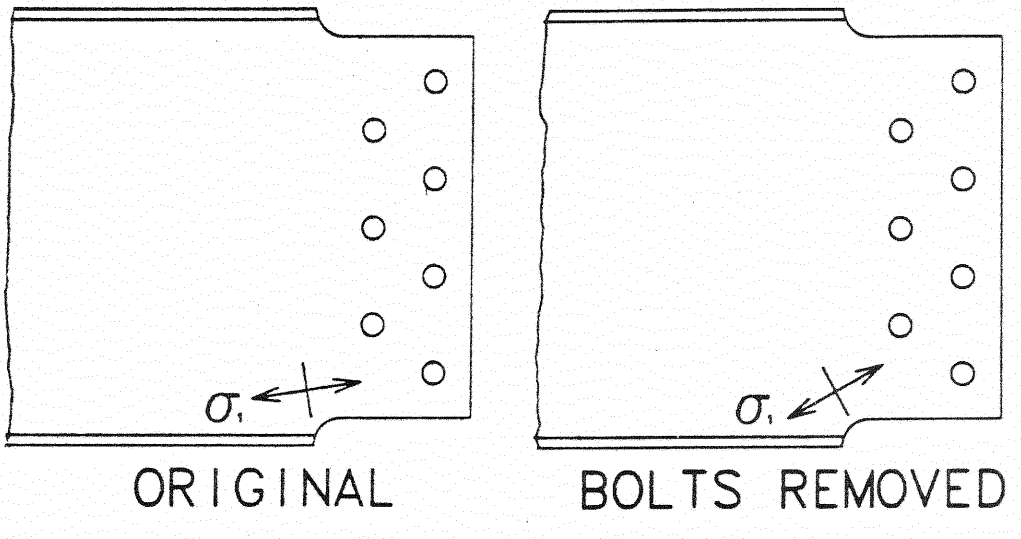

Figure 37. Comparison of Stresses in Original Detail to Stresses With Bolts Removed

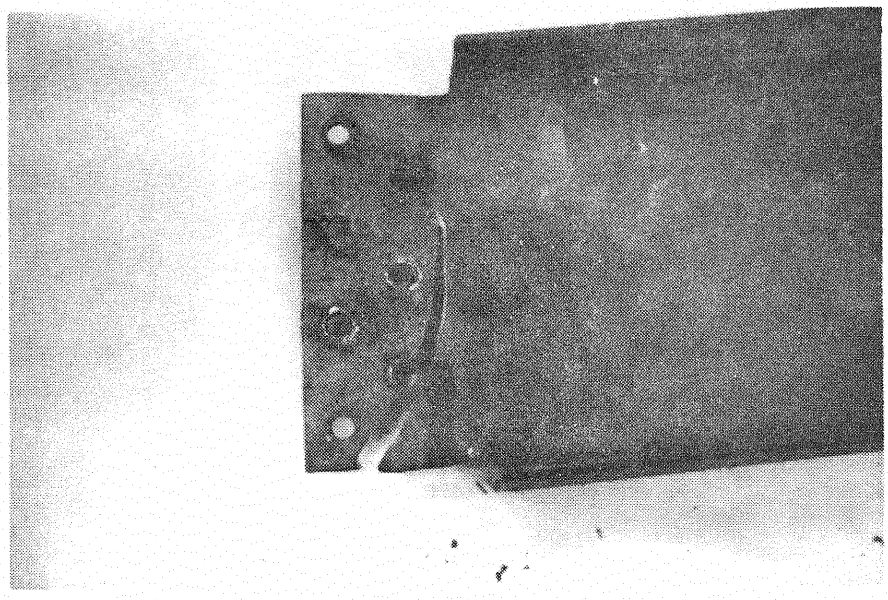

(a)

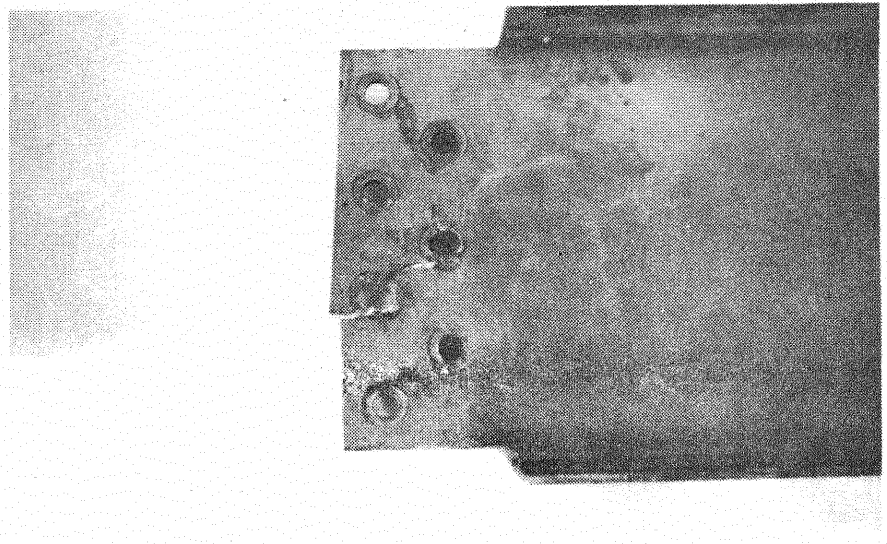

(b)

Figure 38. Failure of Detail With Bolts Removed

each be required to carry a larger percentage of the total moment, but the total moment should not increase (as it does in the laboratory specimens) when two bolts are removed. Laboratory tests on the detail with the bottom two bolts removed are more severe relative to the original detail than are the tests on the other modifications.

Tests were also conducted on precracked specimens. Two original details were cycled with all bolts in place until a crack approximately one inch long could be identified. The test was then stopped so that the bottom two bolts in the connection could be removed, after which the test was continued. No further growth from the one inch cracks was observed after the bolts were removed. Failure in the specimens resulted from cracks initiating in the bolt holes in the same manner as when the entire test was conducted with the bottom two bolts removed. Additional fatigue life for the two test specimens after bolts were removed was 156,210 and 188,650, as compared to an average total fatigue life of 217,950 cycles for the original detail tested at the same range.

Test results indicate that removing the bottom two bolts from the diaphragm-to-girder connection is an effective and reliable way of increasing diaphragm fatigue life. The method is effective even when small cracks are present in the diaphragm at the cope. Laboratory tests on this modification may be more severe than the detail would experience in actual service.

Auxiliary Flange. The auxiliary flange is installed to carry a portion of the load past the cope and reduce the stress in the cope area [3]. A problem with applying this technique to the current situation is that the gusset connection does not allow the auxiliary flange to extend ahead of the cope far enough to help relieve a large portion of the stress.

Tests with the auxiliary flange were conducted on specimens having fatigue cracks which had propagated approximately 3/4 in. prior to any modifications being performed. A 1/2-in. diameter hole was drilled at the end of the crack to help retard crack growth. This hole size was selected to match the size used in Reference [4]. The auxiliary flange was then welded in place above the drilled hole.

As can be seen in Table 3 and Figure 35, the modification did increase average specimen fatigue life, but there is a great deal of scatter in the data. In both tests, a short period of no growth after the modification was followed by propagation around the end of the auxiliary flange. A failed specimen is shown in Figure 39. The fact that the crack easily propagated around the auxiliary flange is an indication that the flange does not extend far enough ahead of the cope to be effective.

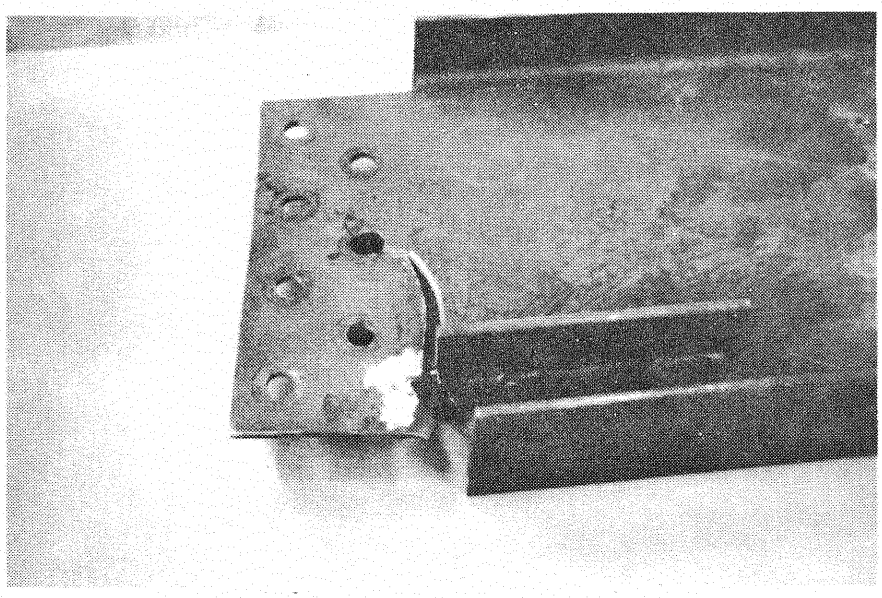

Figure 39. Failure of the Auxiliary Flange Detail

CHAPTER 5

SUMMARY AND CONCLUSIONS

5.1 Field Tests

The pattern of cracked diaphragms and the location of cracks in the diaphragms indicate that diaphragms at each transverse location between the piers are acting as continuous beams. In all but one case, the cracks originate in the bottom flange cope and grow up through the web. No cracks were found at connections to exterior girders. Taken as a whole, these observations indicate that the "continuous" diaphragms are being loaded by the differential deflections of the longitudinal girders.

A truck in one of the traffic lanes will cause the interior girders to deflect more than the exterior girders. This in turn will cause the "continuous" diaphragm to deflect more at the interior of the bridge than at the exterior, inducing high positive moments at the interior region. Exterior girders are not stiff enough torsionally to induce high negative moments when the load is near the diaphragm midspan. The positive moment produces tension in the bottom flange which is magnified by the stress concentration at the cope.

The one case where cracks were found in the upper cope is also the one case where cracks were found in diaphragms above pier caps. At this location, girders are restrained from translating vertically by the pier caps and are restrained from rotating about their longitudinal axes by the slab and the pier caps. Hence, the girders act almost as fixed supports for the diaphragms. Wheel loads acting through the slab produce tension at the top and compression at the bottom of the diaphragm ends. The result is a crack growing in the upper cope rather than the lower cope. Since cracking occurs

at the top cope in only one diaphragm, the stress range or the number of cycles experienced by individual top copes must be less than experienced by bottom copes.

Measured strains tended to be very low, making it difficult to precisely describe deformation patterns and load paths in the bridge. There are sufficient data to conclude, in support of the statements made above, that the diaphragms are being loaded by displacements of the girders. Plots of strain versus truck position show that the diaphragms are loaded when a truck moves onto the span containing that diaphragm. Strain in the diaphragm increases as the truck approaches the diaphragm, reaches a maximum when the truck is at the same longitudinal position as the diaphragm, and decreases as the truck moves away from the diaphragm.

5.2 Analysis

The bridge superstructure was analyzed by treating the steel frame as a grid with the piers acting as simple supports. To account for the concrete deck, moments of inertia for grid members were calculated assuming the girders and diaphragms are fully composite with the deck. Wheel loads from the tank truck were applied to grid members. Stresses calculated using moments from these grid analyses exhibited a variation with truck position similar to the variations observed in field testing.

Finite element analyses were used to compare stresses in the original diaphragm detail to stresses in modified details. Stresses at the cope are slightly reduced by tapering the cope or more significantly reduced by removing the bottom bolts from the connection. Stresses in the diaphragm are most effectively reduced by not coping the bottom flange.

5.3 Laboratory Tests

Physical and chemical properties of the diaphragm steel were measured. Both chemical analysis and tension tests indicate that, as specified in the original drawings, the steel satisfies ASTM Standard A36. Charpy tests show that the impact resistance of the steel satisfies AASHTO bridge specifications.

Fatigue test results indicate that the original connection is an AASHTO category D detail, and that fatigue performance can be improved by tapering the cope, installing an auxiliary flange, removing the bottom two bolts from the connection, or not coping the bottom flange. Not coping the bottom flange produced the greatest improvement in fatigue life. The other three modifications produced approximately the same increase in fatigue life, on the average. Performance of the specimens with the bottom bolts removed was more consistent than performance of the specimens with tapered copes or with auxiliary flanges. Additional tests were run on specimens with small cracks already present in the copes when the bottom bolts were removed. Growth at these initial crack sites stopped and failure eventually occurred as the result of cracks originating from bolt holes.

5.4 Recommendations

It is recommended that for uncracked diaphragms and for diaphragms with cracks shorter than one inch, the bottom two bolts in the diaphragm-to-girder connection be removed. This recommendation is based on the effectiveness of this modification to increase fatigue life--even for diaphragms containing small cracks--and the relative ease with which this modification can be accomplished. Diaphragms containing cracks longer than one inch should be removed and replaced with diaphragms not coped at the bottom

flange. To encourage a smooth flow of stress from one diaphragm to the next, the bottom two bolts should also be omitted from the uncoped diaphragms.

Since the diaphragms do not contribute substantially to the overall stiffness of the bridge, the slight reduction in diaphragm stiffness caused by removing two bolts from the connection should not result in substantial changes in load distribution patterns in main members. Diaphragms cracked over a portion of their depth experience a reduction in stiffness similar to the reduction resulting from removing bottom bolts, and there is no evidence that damage patterns in nearby members are altered by the decrease in stiffness of cracked diaphragms.

REFERENCES

1. American Association of State Highway and Transportation Officials. Standard Specifications for Highway Bridges. 13th Ed. Washington, DC, 1983.

2. Cudney, G. R. "Stress Histories of Highway Bridges." Proceedings, Journal of the Structural Division, ASCE, Vol. 94, No. ST12 (Dec. 1968), pp. 2725-2737.

3. Fisher, J. W. Bridge Fatigue Guide--Design and Details. American Institute of Steel Construction, 1977.

4. Fisher, J. W., H. Hausammann, M. D. Sullivan, and A. W. Pense. Detection and Repair of Fatigue Damage in Welded Highway Bridges. National Cooperative Highway Research Program Report 206. Washington, DC: Transportation Research Board, June 1979.

5. ICES STRUDL--II, Engineering User's Manual. Cambridge: Massachusetts Institute of Technology, 1971.

6. Keating, P. B., and J. W. Fisher. "Fatigue Behavior of Variable Loaded Bridge Details Near the Fatigue Limit." Transportation Research Record 1118. Transportation Research Board (1987), pp. 56-64.

7. Walker, W. H., and A. S. Velestos. Response of Simple-Span Highway Bridges to Moving Vehicles. Bulletin 486. Engineering Experiment Station, University of Illinois, 1966.

8. Walker, W. H. "Lateral Load Distribution on Multi-Girder Bridges." Proceedings, National Engineering Conference, Nashville, TN, June 1986, pp. 341-1-34-17.

APPENDIX A

MATERIAL PROPERTIES

TABLE 4

CHEMICAL PROPERTIES OF WIDE FLANGE

Element	Composition in Percent	ASTM Limits in Percent
Carbon	0.230	0.26 max
Manganese	0.560	---
Phosphorous	0.007	0.04 max
Sulfur	0.018	0.05 max
Silicon	0.070	---
Nickel	0.020	---
Chromium	0.060	---
Molybdenum	<0.010	---
Copper	0.030	---

TABLE 5

TENSION TEST RESULTS

	Yield Strength (KSI)	Ultimate Tensile Strength (KSI)	Elongation at Fracture* (%)
Flange	38.8	61.2	44
Web	45.3	61.7	44
ASTM Limits	36 min.	58 min.-80 max.	20 min.

*8-in. gage length.

TABLE 6

DATA FROM CHARPY IMPACT TESTS

Material Specimens	Temperature (°C)	Energy (Ft-Lbs)
Flange	-74	1.0
	-21	15.5
	0	15.0
	7	42.0
	12	59.5
	20	57.5
	25	65.0
	96	73.0
Web	-74	1.0
	0	38.0
	25	38.5
	96	40.0

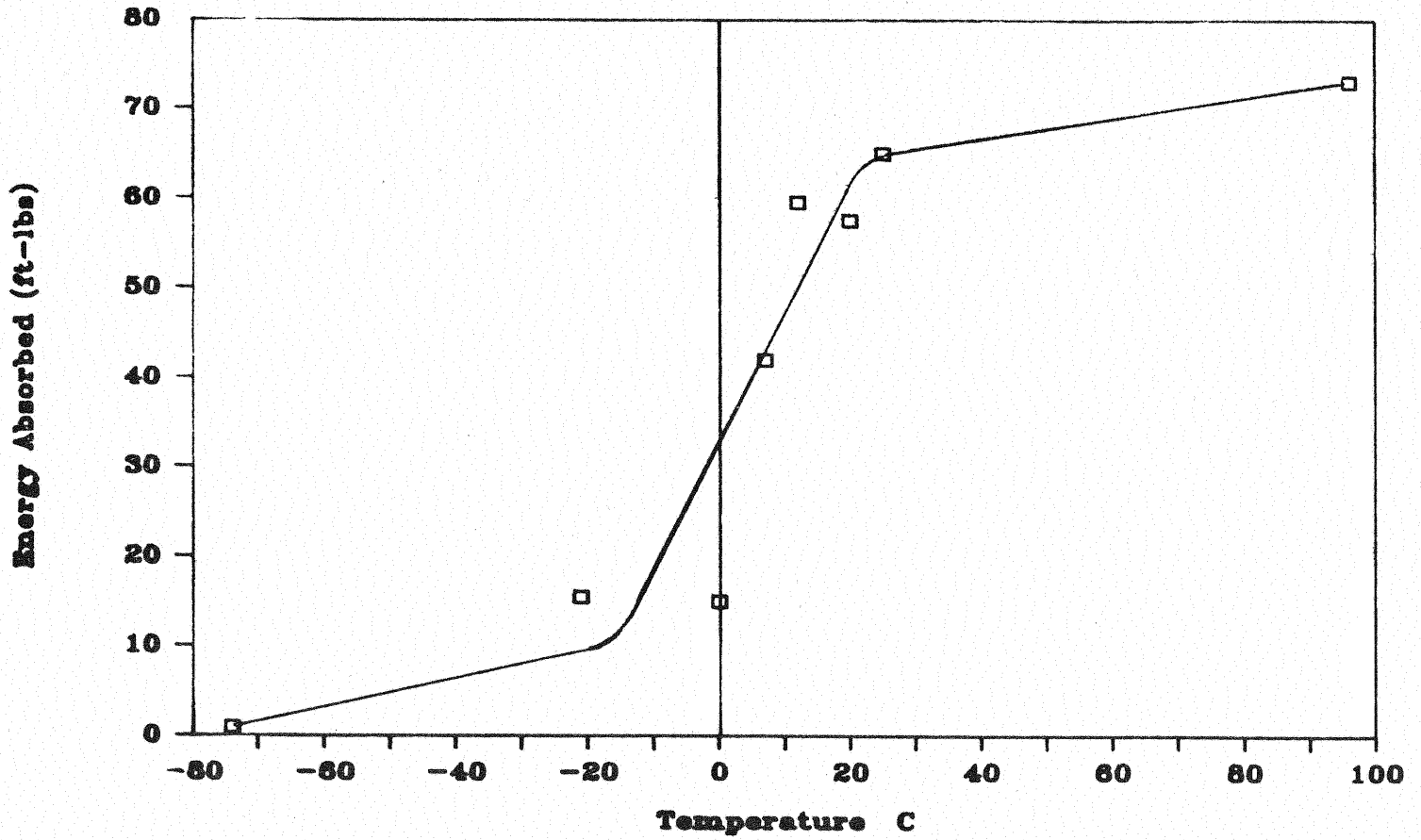

Figure 40. Charpy Impact Test Data for Beam Flange

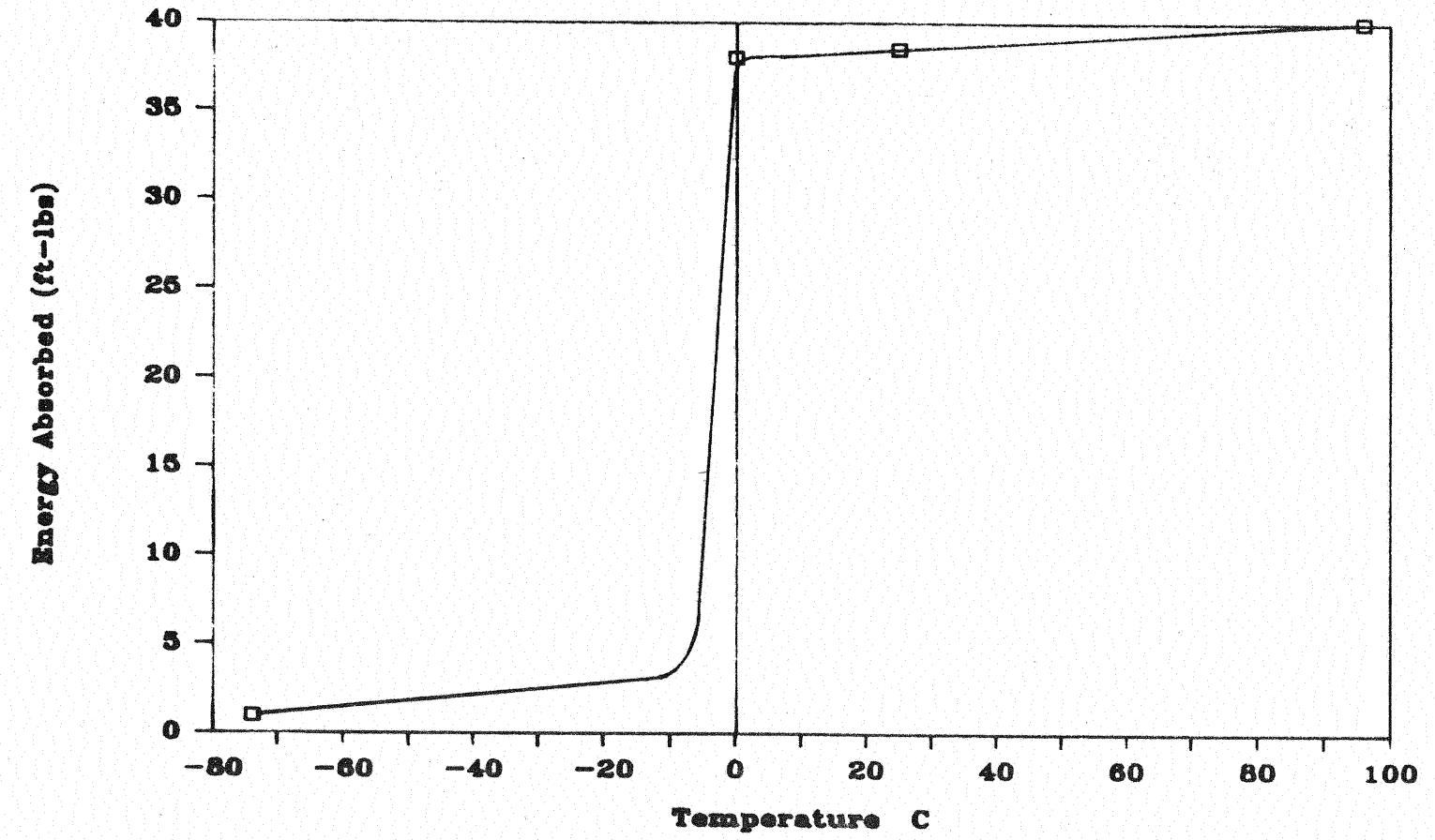

Figure 41. Charpy Impact Test Data for Beam Web

APPENDIX B

CAPACITY OF CONNECTION

WITH BOLTS REMOVED

Check diaphragm-to-girder connection capacity when two bolts are removed from the seven-bolt connection.

Bolt Shear (Using 3/4 in. Diameter, A325 Bolts, Friction Connections)

$$\text{Capacity} = (7.7\ \text{K/bolt})(5\ \text{bolts}) = 38.5^{k}$$

Bearing

Check bearing even though this is a friction connection. The web thickness for a W16x26 is 0.25 in. The gusset plate thickness is 0.375 in. Therefore, the web of the W16x26 will control bearing capacity.

$$\text{Capacity} = (1.2\ F_u)(t_w)(d_{bolt})(\text{No. bolts})$$

$$\text{Capacity} = (1.2)(58\ \text{ksi})(0.25")(0.75")(5\ \text{bolts})$$

$$\text{Capacity} = 65^{k}$$

The total rear axle load from an HS20 truck is 32^{k}, which is less than both the bolt shear capacity and the bearing capacity. The connection is adequate with only five bolts.

Capacity calculations are performed according to the American Institute of Steel Construction's Manual of Steel Construction, 8th Edition.